

B meson rare decays in the TNMSSM

Hai-Xiang Chen^{a*}, Sheng-Kai Cui^a, Ning-Yu Zhu^a, Zhao-Yang Zhang^a, Huai-Cong Hu^a

^a*Department of Physics, Guangxi University, Nanning, 530004, China*

Abstract

We investigate the two loop electroweak corrections to B meson rare decays $\bar{B} \rightarrow X_s \gamma$ and $B_s^0 \rightarrow \mu^+ \mu^-$ in the minimal supersymmetry standard model (MSSM) extension with two triplets and one singlet (TNMSSM). The new particle contents and interactions in the TNMSSM can affect the theoretical predictions of the branching ratios $\text{Br}(\bar{B} \rightarrow X_s \gamma)$ and $\text{Br}(B_s^0 \rightarrow \mu^+ \mu^-)$, and the corrections from two loop diagrams to the process $\bar{B} \rightarrow X_s \gamma$ can reach around 4%. Considering the latest experimental measurements, the numerical results of $\text{Br}(\bar{B} \rightarrow X_s \gamma)$ and $\text{Br}(B_s^0 \rightarrow \mu^+ \mu^-)$ in the TNMSSM are presented and analyzed. It is found that the results in the TNMSSM can fit the updated experimental data well and the new parameters T_λ , κ , λ affect the theoretical predictions of $\text{Br}(\bar{B} \rightarrow X_s \gamma)$ and $\text{Br}(B_s^0 \rightarrow \mu^+ \mu^-)$ obviously.

PACS numbers: 12.60.Jv, 13.20.He

Keywords: Supersymmetry, B physics, Rare decays

* haixchen@hotmail.com

I. INTRODUCTION

After the discovery of Higgs on the Large Hadron Collider (LHC) in 2012, all particles predicted by the SM have been found. However, there are still some problems that are difficult to be solved by the SM, such as the non-zero neutrino mass, reasonable dark matter candidates and etc. It indicates new physics is needed to extend the SM. And since B meson rare decay processes $\bar{B} \rightarrow X_s \gamma$ and $B_s^0 \rightarrow \mu^+ \mu^-$ are not affected by the uncertainties of non-perturbative QCD, research on B physics is particularly sensitive to exploring new physical effects beyond the SM. In Refs. [1–4], the average experimental data on the branching ratios of $\bar{B} \rightarrow X_s \gamma$ and $B_s^0 \rightarrow \mu^+ \mu^-$ are provided as

$$\begin{aligned} \text{Br}(\bar{B} \rightarrow X_s \gamma) &= (3.49 \pm 0.19) \times 10^{-4}, \\ \text{Br}(B_s^0 \rightarrow \mu^+ \mu^-) &= (2.9_{-0.6}^{+0.7}) \times 10^{-9}. \end{aligned} \quad (1)$$

The branching ratios of $\bar{B} \rightarrow X_s \gamma$ and $B_s^0 \rightarrow \mu^+ \mu^-$ predicted by the SM are [5–13]

$$\begin{aligned} \text{Br}(\bar{B} \rightarrow X_s \gamma)_{\text{SM}} &= (3.36 \pm 0.23) \times 10^{-4}, \\ \text{Br}(B_s^0 \rightarrow \mu^+ \mu^-)_{\text{SM}} &= (3.23 \pm 0.27) \times 10^{-9}, \end{aligned} \quad (2)$$

which coincides with the experimental data very well. Therefore, the new physics contributions to $\bar{B} \rightarrow X_s \gamma$ and $B_s^0 \rightarrow \mu^+ \mu^-$ are limited strictly by the accurate measurements on the processes $\bar{B} \rightarrow X_s \gamma$ and $B_s^0 \rightarrow \mu^+ \mu^-$.

As one of the most famous extensions of the SM, the B meson rare decay process $\bar{B} \rightarrow X_s \gamma$ is analyzed in the MSSM [14–21]. In 1998, Ciuchini presented the QCD corrections to $\bar{B} \rightarrow X_s \gamma$ at Next-to-leading order (NLO) in the Two-Higgs doublet model (THDM) [22]. Then, the two loop QCD corrections was proposed in Ref. [23]. Not only the process $\bar{B} \rightarrow X_s \gamma$, there are also many references researching on other B meson rare decay processes in the THDM [24–29]. Recently, the authors of Refs. [30–40] have discussed the supersymmetric effects on the B meson rare decay processes. Meanwhile, Long et al present the computation of the flavor transition process $b \rightarrow s \gamma$ [41]. The authors of Ref. [42] have investigated the two aspects of hadronic B decays, and then these processes in the case of CP violation have been discussed [43]. Moreover, many possibilities for searching supersymmetry effects in

different B meson rare decay processes have been proposed [44–46]. When investigating the processes of rare B decay, the supersymmetry effects are very interesting, and B decay can be conducive for us to understand the characteristics of the supersymmetry model in detail while limiting the parameter space [47, 48].

TNMSSM is an extension of Next-to minimal supersymmetric standard model (NMSSM) containing two $SU(2)_L$ triplets with hypercharge ± 1 , where the NMSSM introduces an additional scalar singlet compared with the MSSM [49]. The new scalar singlet in the NMSSM is introduced to solve the μ problem in the MSSM [50, 51]. However, NMSSM fails to improve the little hierarchy problem [52–57]. Fortunately, the author of Ref. [49] solved these problems in the TNMSSM by introducing two scalar triplets which are responsible for large correction to the lightest physical Higgs mass. The tiny neutrino mass measured at the neutrino oscillation experiments can be obtained by applying type II seesaw mechanism and a discrete flavor symmetry G_F in TNMSSM (i.e. the flavored-TNMSSM) [58]. In this work, we analyze the two loop electroweak corrections to $\bar{B} \rightarrow X_s \gamma$ and $B_s^0 \rightarrow \mu^+ \mu^-$ in the TNMSSM. Compared with the MSSM, new particle contents and interactions can make important contributions to the processes.

The paper is organized as follows. The superpotential, the soft breaking terms and the mass matrices of singly-charged Higgs and CP-even Higgs in the TNMSSM are reviewed briefly in Sec.II. Sec.III and Sec.IV give the corresponding Wilson coefficients and analytic expressions for $\text{Br}(\bar{B} \rightarrow X_s \gamma)$ and $\text{Br}(B_s^0 \rightarrow \mu^+ \mu^-)$. Sec.V analyses the numerical results and Sec.VI gives a summary. The corresponding matrix elements and the concrete expressions of the Wilson coefficients are collected in the appendices.

II. THE TNMSSM

There are different versions of TNMSSM, such as the type of a triplet with hypercharge $Y = 0$ [59–61]. Here we adopt the version of two triplets with hypercharge ± 1 to keep on our work. As mentioned before, the TNMSSM contains two $SU(2)_L$ triplets $\hat{T} \sim (1, 3, 1)$, $\hat{\bar{T}} \sim (-1, 3, 1)$ with $Y = \pm 1$ and a SM gauge singlet $\hat{S} \sim (0, 1, 1)$. For the mass matrices and the interaction vertexes needed, we encode this version of TNMSSM in SARAH [62–66].

The chiral superfields for quarks and leptons are given by

$$\begin{aligned}\hat{Q} &= \begin{pmatrix} \hat{U} \\ \hat{D} \end{pmatrix} \sim (1/6, 2, 3), & \hat{L} &= \begin{pmatrix} \hat{\nu} \\ \hat{E} \end{pmatrix} \sim (-1/2, 2, 1), \\ \hat{U}^c &\sim (-2/3, 1, 3), & \hat{D}^c &\sim (1/3, 1, 3), & \hat{E}^c &\sim (1, 1, 1),\end{aligned}\quad (3)$$

where we ignore the index of generations and the quantum numbers of $U(1)_Y$, $SU(2)_L$ and $SU(3)_C$ are indicated in the bracket, respectively. Additionally, the expressions and the quantum numbers of two Higgs triplets, two doublets and one singlet are assigned as

$$\begin{aligned}\hat{T} &= \begin{pmatrix} \frac{1}{\sqrt{2}}T^+, & -T^{++} \\ T^0, & \frac{-1}{\sqrt{2}}T^+ \end{pmatrix} \sim (1, 3, 1), & \hat{\bar{T}} &= \begin{pmatrix} \frac{1}{\sqrt{2}}\bar{T}^-, & -\bar{T}^0 \\ \bar{T}^{--}, & \frac{-1}{\sqrt{2}}\bar{T}^- \end{pmatrix} \sim (-1, 3, 1), \\ \hat{H}_d &= \begin{pmatrix} H_d^0 \\ H_d^- \end{pmatrix} \sim (-1/2, 2, 1), & \hat{H}_u &= \begin{pmatrix} H_u^+ \\ H_u^0 \end{pmatrix} \sim (1/2, 2, 1), & \hat{S} &\sim (0, 1, 1).\end{aligned}\quad (4)$$

In the previous expressions, T^0 and \bar{T}^0 are two complex neutral superfields, while T^+ , \bar{T}^- are singly-charged Higgs and T^{++} , \bar{T}^{--} are doubly-charged Higgs.

The superpotential of the TNMSSM W_{TNMSSM} contains two parts

$$W_{\text{TNMSSM}} = W_{\text{MSSM}} + W_{\text{TS}}, \quad (5)$$

with

$$W_{\text{MSSM}} = Y_u \hat{U}^c \hat{H}_u \cdot \hat{Q} - Y_d \hat{D}^c \hat{H}_d \cdot \hat{Q} - Y_e \hat{E}^c \hat{H}_d \cdot \hat{L}, \quad (6)$$

where W_{MSSM} is the superpotential of the MSSM, and W_{TS} explains the extended scalar sector including two triplets and a SM gauge singlet,

$$W_{\text{TS}} = \chi_d \hat{H}_d \cdot \hat{T} \hat{H}_d + \chi_u \hat{H}_u \cdot \hat{\bar{T}} \hat{H}_u + \frac{1}{3} \kappa \hat{S} \hat{S} \hat{S} + \lambda \hat{S} \hat{H}_u \cdot \hat{H}_d + \Lambda_T \hat{S} \text{Tr}(\hat{T} \hat{T}). \quad (7)$$

Here, we also neglect the index of generations. From Eq.(6), we could find that there are only two MSSM Higgs doublets coupled with fermion multiplet via Yukawa coupling. Then, the general soft breaking terms are given by

$$\begin{aligned}-\mathcal{L}_{\text{soft}} &= m_{H_u}^2 |H_u|^2 + m_{H_d}^2 |H_d|^2 + m_S^2 |S|^2 + m_T^2 \text{Tr}(|T|^2) + m_{\bar{T}}^2 \text{Tr}(|\bar{T}|^2) \\ &+ m_Q^2 |Q|^2 + m_U^2 |U|^2 + m_D^2 |D|^2 + (T_{\Lambda_T} S \text{Tr}(T \bar{T}) + T_\lambda S H_u \cdot H_d + \frac{1}{3} T_\kappa S^3 \\ &- T_{\chi_u} H_u \cdot \bar{T} H_u - T_{\chi_d} H_d \cdot T H_d + T_{u,ij} \tilde{Q}_j \cdot H_u \tilde{U}_i^c - T_{d,ij} \tilde{Q}_j \cdot H_d \tilde{D}_i^c + H.c.),\end{aligned}\quad (8)$$

where

$$H_u \cdot H_d = H_u^+ H_d^- - H_u^0 H_d^0, \quad (9)$$

$$H_d \cdot T H_d = \sqrt{2} H_d^- H_d^0 T^+ - (H_d^0)^2 T^0 - (H_d^-)^2 T^{++}, \quad (10)$$

$$H_u \cdot \bar{T} H_u = \sqrt{2} H_u^+ H_u^0 \bar{T}^- - (H_u^0)^2 \bar{T}^0 - (H_u^+)^2 \bar{T}^{--}. \quad (11)$$

When the Z_3 symmetry is imposed, the μ term only forms after the singlet S has obtained a vacuum expectation value (VEV) v_S as $\mu = \frac{1}{\sqrt{2}} \lambda v_S$. The coefficients in the Higgs sector are assumed to be real in the following calculations.

The $SU(2)_L \otimes U(1)_Y$ electroweak symmetry breaking occurs when the neutral parts of Higgs fields obtain the VEVs

$$\begin{aligned} H_d^0 &= \frac{1}{\sqrt{2}}(v_d + \Re H_d^0 + i\Im H_d^0), & H_u^0 &= \frac{1}{\sqrt{2}}(v_u + \Re H_u^0 + i\Im H_u^0), \\ T^0 &= \frac{1}{\sqrt{2}}(v_T + \Re T^0 + i\Im T^0), & \bar{T}^0 &= \frac{1}{\sqrt{2}}(v_{\bar{T}} + \Re \bar{T}^0 + i\Im \bar{T}^0), \\ S &= \frac{1}{\sqrt{2}}(v_S + \Re S + i\Im S). \end{aligned} \quad (12)$$

Meanwhile, the VEVs of the triplets must to be small to avoid large ρ parameter correction [49] and the VEV of the singlet is required to be large for generating a large μ term like the case in the NMSSM [50]. In the TNMSSM, the mass of Z gauge boson reads

$$M_Z^2 = \frac{1}{4}(g_1^2 + g_2^2)(v_u^2 + v_d^2 + 4v_T^2 + 4v_{\bar{T}}^2) = \frac{1}{4}(g_1^2 + g_2^2)v^2, \quad (13)$$

where g_1 and g_2 represent the gauge coupling constants of $U(1)_Y$ and $SU(2)_L$ respectively. It will be seen from this that due to the triplets, the electroweak symmetry breaking VEV for the doublets compared to MSSM is changed as

$$v = \sqrt{v_u^2 + v_d^2 + 4v_T^2 + 4v_{\bar{T}}^2} \approx 246 \text{ GeV}. \quad (14)$$

Minimizing the Higgs scalar potential

$$\frac{\partial V}{\partial v_u} = \frac{\partial V}{\partial v_d} = \frac{\partial V}{\partial v_T} = \frac{\partial V}{\partial v_{\bar{T}}} = \frac{\partial V}{\partial v_S} = 0, \quad (15)$$

we can deduce the squared mass matrices of the neutral Higgs and singly-charged Higgs. In the basis $(H_d^-, H_u^{+,*}, \bar{T}^-, T^{+,*})$ and $(H_d^{-,*}, H_u^+, \bar{T}^{-,*}, T^+)$, the squared mass matrix for

singly-charged Higgs can be expressed as

$$M_{H^\pm}^2 = \begin{pmatrix} m_{H_d^- H_d^-,*} & m_{H_u^+,* H_d^-,*} & m_{\bar{T}^- H_d^-,*} & m_{T^+,* H_d^-,*} \\ m_{H_d^- H_u^+} & m_{H_u^+,* H_u^+} & m_{\bar{T}^- H_u^+} & m_{T^+,* H_u^+} \\ m_{H_d^- \bar{T}^-,*} & m_{H_u^+,* \bar{T}^-,*} & m_{\bar{T}^- \bar{T}^-,*} & m_{T^+,* \bar{T}^-,*} \\ m_{H_d^- T^+} & m_{H_u^+,* T^+} & m_{\bar{T}^- T^+} & m_{T^+,* T^+} \end{pmatrix}. \quad (16)$$

The 4×4 squared mass matrix in Eq.(16) can be diagonalized by the unitary matrix Z^{H^\pm}

$$Z^{H^\pm} M_{H^\pm}^2 Z^{H^\pm,\dagger} = M_{H^\pm,diag}^2. \quad (17)$$

Then, we can get three mass eigenstates $(H_1^\pm, H_2^\pm, H_3^\pm)$ for singly-charged Higgs and one state G^\pm for the massless Goldstone boson. Therefore, the TNMSSM has two more singly-charged Higgs due to the triplets, with respect to MSSM. These new defined singly-charged Higgs will bring contributions to loop corrections for $\bar{B} \rightarrow X_s \gamma$ and $B_s^0 \rightarrow \mu^+ \mu^-$.

At tree level, the squared mass matrix for CP-even Higgs is given in the basis $(\Re H_d^0, \Re H_u^0, \Re S, \Re T^0, \Re \bar{T}^0)$ as

$$M_h^2 = \begin{pmatrix} m_{H_d^0 H_d^0} & m_{H_u^0 H_d^0} & m_{S H_d^0} & m_{T^0 H_d^0} & m_{\bar{T}^0 H_d^0} \\ m_{H_d^0 H_u^0} & m_{H_u^0 H_u^0} & m_{S H_u^0} & m_{T^0 H_u^0} & m_{\bar{T}^0 H_u^0} \\ m_{H_d^0 S} & m_{H_u^0 S} & m_{SS} & m_{T^0 S} & m_{\bar{T}^0 S} \\ m_{H_d^0 T^0} & m_{H_u^0 T^0} & m_{S T^0} & m_{T^0 T^0} & m_{\bar{T}^0 T^0} \\ m_{H_d^0 \bar{T}^0} & m_{H_u^0 \bar{T}^0} & m_{S \bar{T}^0} & m_{T^0 \bar{T}^0} & m_{\bar{T}^0 \bar{T}^0} \end{pmatrix}. \quad (18)$$

The corresponding matrix elements of the squared mass matrices for singly-charged Higgs and CP-even Higgs are collected in Appendix A.

Including the leading-log radiative corrections up to two loops for stop and top sector [67–69], the mass of the SM-like Higgs boson can be written as

$$\begin{aligned} m_h &= \sqrt{(m_{h_1}^0)^2 + \Delta m_h^2}, \\ \Delta m_h^2 &= \frac{3m_t^4}{2\pi v^2} \left[\left(\tilde{t} + \frac{1}{2} + \tilde{X}_t \right) + \frac{1}{16\pi^2} \left(\frac{3m_t^2}{2v^2} - 32\pi\alpha_3 \right) (\tilde{t}^2 + \tilde{X}_t \tilde{t}) \right], \\ \tilde{t} &= \log \frac{M_S^2}{m_t^2}, \quad \tilde{X}_t = \frac{2\tilde{A}_t^2}{M_S^2} \left(1 - \frac{\tilde{A}_t^2}{12M_S^2} \right), \end{aligned} \quad (19)$$

where $m_{h_1}^0$ is the lightest tree-level Higgs boson mass, α_3 is the running QCD coupling constant, $M_S = \sqrt{m_{\tilde{t}_1} m_{\tilde{t}_2}}$ is the geometric mean of the stop masses $m_{\tilde{t}_{1,2}}$, m_t is the top quark pole mass, and $\tilde{A}_t = A_t - \mu \cot \beta$ with $A_t = T_{u,33}$ being the trilinear Higgs stop coupling.

In the basis $(\tilde{u}_L, \tilde{u}_R)$ and $(\tilde{d}_L, \tilde{d}_R)$, we can obtain the squared mass matrices for Up-Squark and Down-Squark as

$$m_{\tilde{u}}^2 = \begin{pmatrix} m_{\tilde{u}_L \tilde{u}_L^*} & m_{\tilde{u}_R \tilde{u}_L^*}^\dagger \\ m_{\tilde{u}_L \tilde{u}_R^*} & m_{\tilde{u}_R \tilde{u}_R^*} \end{pmatrix}, \quad (20)$$

$$m_{\tilde{d}}^2 = \begin{pmatrix} m_{\tilde{d}_L \tilde{d}_L^*} & m_{\tilde{d}_R \tilde{d}_L^*}^\dagger \\ m_{\tilde{d}_L \tilde{d}_R^*} & m_{\tilde{d}_R \tilde{d}_R^*} \end{pmatrix}, \quad (21)$$

where

$$\begin{aligned} m_{\tilde{u}_L \tilde{u}_L^*} &= -\frac{1}{24}(-3g_2^2 + g_1^2)(2v_T^2 - 2v_T^2 - v_u^2 + v_d^2) + \frac{1}{2}(2m_q^2 + v_u^2 Y_u^\dagger Y_u), \\ m_{\tilde{u}_L \tilde{u}_R^*} &= \frac{1}{2}(\sqrt{2}v_u T_u + Y_u(2\chi_u v_u v_T - \lambda v_d v_S)), \\ m_{\tilde{u}_R \tilde{u}_R^*} &= \frac{1}{6}g_1^2(2v_T^2 - 2v_T^2 - v_u^2 + v_d^2) + \frac{1}{2}(2m_u^2 + v_u^2 Y_u Y_u^\dagger), \\ m_{\tilde{d}_L \tilde{d}_L^*} &= -\frac{1}{24}(3g_2^2 + g_1^2)(2v_T^2 - 2v_T^2 - v_u^2 + v_d^2) + \frac{1}{2}(2m_q^2 + v_d^2 Y_d^\dagger Y_d), \\ m_{\tilde{d}_L \tilde{d}_R^*} &= \frac{1}{2}(\sqrt{2}v_d T_d + Y_d(2\chi_d v_d v_T - \lambda v_u v_S)), \\ m_{\tilde{d}_R \tilde{d}_R^*} &= \frac{1}{12}g_1^2(-2v_T^2 + 2v_T^2 + v_u^2 - v_d^2) + \frac{1}{2}(2m_d^2 + v_d^2 Y_d Y_d^\dagger). \end{aligned} \quad (22)$$

III. RARE DECAY $\bar{B} \rightarrow X_s \gamma$

The effective Hamilton for the transition $b \rightarrow s$ at hadronic scale can be described by

$$\begin{aligned} H_{eff} &= -\frac{4G_F}{\sqrt{2}} V_{ts}^* V_{tb} \left[C_1 \mathcal{O}_1^c + C_2 \mathcal{O}_2^c + \sum_{i=3}^6 \mathcal{O}_i + \sum_{i=7}^{10} (C_i \mathcal{O}_i + C'_i \mathcal{O}'_i) \right. \\ &\quad \left. + \sum_{i=S,P} (C_i \mathcal{O}_i + C'_i \mathcal{O}'_i) \right]. \end{aligned} \quad (23)$$

From the Refs. [70–75], $\mathcal{O}_i (i = 1, \dots, 10, S, P)$ and $\mathcal{O}'_i (i = 7, \dots, 10, S, P)$ are defined as

$$\mathcal{O}_1^c = (\bar{s}_L \gamma_\mu T^a u_L)(\bar{u}_L \gamma^\mu T^a b_L), \quad \mathcal{O}_2^c = (\bar{s}_L \gamma_\mu u_L)(\bar{u}_L \gamma^\mu b_L),$$

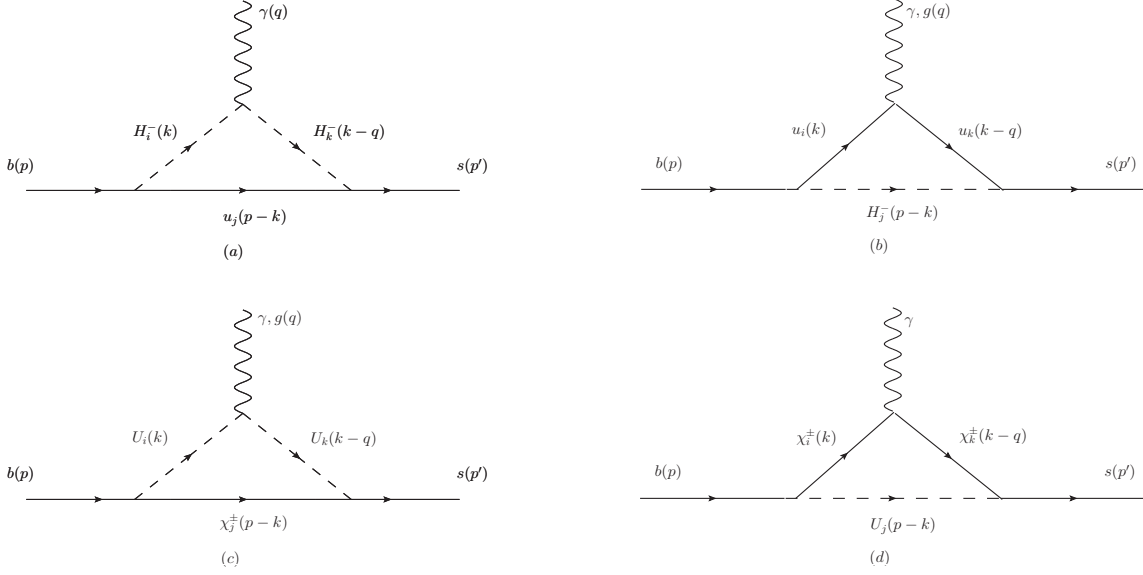


FIG. 1: The one loop Feynman diagrams contributing to $\bar{B} \rightarrow X_s \gamma$ in the TNMSSM.

$$\begin{aligned}
\mathcal{O}_3 &= (\bar{s}_L \gamma_\mu b_L) \sum_q (\bar{q} \gamma^\mu q), \quad \mathcal{O}_4 = (\bar{s}_L \gamma_\mu T^a b_L) \sum_q (\bar{q} \gamma^\mu T^a q), \\
\mathcal{O}_5 &= (\bar{s}_L \gamma_\mu \gamma_\nu \gamma_\rho b_L) \sum_q (\bar{q} \gamma^\mu \gamma^\nu \gamma^\rho q), \quad \mathcal{O}_6 = (\bar{s}_L \gamma_\mu \gamma_\nu \gamma_\rho T^a b_L) \sum_q (\bar{q} \gamma^\mu \gamma^\nu \gamma^\rho T^a q), \\
\mathcal{O}_7 &= \frac{e}{16\pi^2} m_b (\bar{s}_L \sigma_{\mu\nu} b_R) F^{\mu\nu}, \quad \mathcal{O}'_7 = \frac{e}{16\pi^2} m_b (\bar{s}_R \sigma_{\mu\nu} b_L) F^{\mu\nu}, \\
\mathcal{O}_8 &= \frac{g_s}{16\pi^2} m_b (\bar{s}_L \sigma_{\mu\nu} T^a b_R) G^{a,\mu\nu}, \quad \mathcal{O}'_8 = \frac{g_s}{16\pi^2} m_b (\bar{s}_R \sigma_{\mu\nu} T^a b_L) G^{a,\mu\nu}, \\
\mathcal{O}_9 &= \frac{e^2}{g_s^2} (\bar{s}_L \gamma_\mu b_L) \bar{l} \gamma^\mu l, \quad \mathcal{O}'_9 = \frac{e^2}{g_s^2} (\bar{s}_R \gamma_\mu b_R) \bar{l} \gamma^\mu l, \\
\mathcal{O}_{10} &= \frac{e^2}{g_s^2} (\bar{s}_L \gamma_\mu b_L) \bar{l} \gamma^\mu \gamma_5 l, \quad \mathcal{O}'_{10} = \frac{e^2}{g_s^2} (\bar{s}_R \gamma_\mu b_R) \bar{l} \gamma^\mu \gamma_5 l, \\
\mathcal{O}_S &= \frac{e^2}{16\pi^2} m_b (\bar{s}_L b_R) \bar{l} l, \quad \mathcal{O}'_S = \frac{e^2}{16\pi^2} m_b (\bar{s}_R b_L) \bar{l} l, \\
\mathcal{O}_P &= \frac{e^2}{16\pi^2} m_b (\bar{s}_L b_R) \bar{l} \gamma_5 l, \quad \mathcal{O}'_P = \frac{e^2}{16\pi^2} m_b (\bar{s}_R b_L) \bar{l} \gamma_5 l,
\end{aligned} \tag{24}$$

where g_s represents the strong coupling, $F^{\mu\nu}$ is the electromagnetic field strength tensor, $G^{\mu\nu}$ is the gluon field strength tensor, and T^a ($a = 1, \dots, 8$) are the $SU(3)$ generators.

As shown in Fig. 1, the main one loop Feynman diagrams contributing to the process $\bar{B} \rightarrow X_s \gamma$ in the TNMSSM are mediated by newly defined up-squarks, singly-charged Higgs and charginos. Compared to the MSSM, these new definitions of particles will affect the

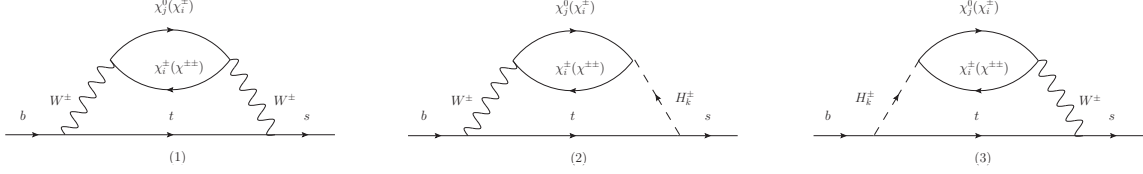


FIG. 2: The relating two loop diagrams in which a closed heavy fermion loop is attached to virtual W^\pm bosons or H^\pm , where a real photon or gluon is attached in all possible ways.

prediction of the process $\bar{B} \rightarrow X_s \gamma$. In the TNMSSM, the one loop Wilson coefficients corresponding to Fig. 1 are $C_{7,NP}^{(a)}(\mu_{EW})$, $C_{7,NP}^{(b)}(\mu_{EW})$, $C_{7,NP}^{(c)}(\mu_{EW})$ and $C_{7,NP}^{(d)}(\mu_{EW})$ and their concrete expressions can be obtained from Appendix B.

At two loop level, we consider the corrections from closed fermion loop in Fig. 2. In Fig. 2, new defined neutralinos, charginos and doubly-charged chargino in the TNMSSM bring new contributions to $\bar{B} \rightarrow X_s \gamma$ compared to the MSSM. Then, the two loop Wilson coefficients $C_{7,NP}^{WW}(\mu_{EW})$, $C_{8,NP}^{WW}(\mu_{EW})$, $C_{7,NP}^{WH}(\mu_{EW})$ and $C_{8,NP}^{WH}(\mu_{EW})$ from Fig. 2 are also collected in Appendix B.

In addition, $C_{8g,NP}(\mu_{EW})$, $C'_{8g,NP}(\mu_{EW})$, $C_{8,NP}^{WW}(\mu_{EW})$, $C_{8,NP}^{WH}(\mu_{EW})$ are Wilson coefficients of the process $b \rightarrow sg$ in the TNMSSM, which can make contributions to the process $b \rightarrow s \gamma$ through the QCD running. Similarly, the Wilson coefficients of the process $b \rightarrow sg$ at EW scale can be written as

$$\begin{aligned}
 C_{8g,NP}(\mu_{EW}) &= [C_{7,NP}^{(b)}(\mu_{EW}) + C_{7,NP}^{(c)}(\mu_{EW})]/Q_u + C_{8,NP}^{WW}(\mu_{EW}) + C_{8,NP}^{WH}(\mu_{EW}), \\
 C'_{8g,NP}(\mu_{EW}) &= C_{8g,NP}(\mu_{EW})(L \leftrightarrow R),
 \end{aligned} \tag{25}$$

where $Q_u = 2/3$.

Based on Wilson coefficients above, the branching ratio of $\bar{B} \rightarrow X_s \gamma$ in the TNMSSM can be given by

$$\text{Br}(\bar{B} \rightarrow X_s \gamma) = R(|C_{7\gamma}(\mu_b)|^2 + N(E_\gamma)), \tag{26}$$

where the overall factor $R = 2.47 \times 10^{-3}$, and the nonperturbative contribution $N(E_\gamma) = (3.6 \pm 0.6) \times 10^{-3}$ [76]. $C_{7\gamma}(\mu_b)$ is defined as

$$C_{7\gamma}(\mu_b) = C_{7\gamma,SM}(\mu_b) + C_{7,NP}(\mu_b), \tag{27}$$

where we choose the hadron scale $\mu_b = 2.5$ GeV and at NNLO level the SM contribution is $C_{7\gamma,SM}(\mu_b) = -0.3689$ [76–79]. The Wilson coefficients for new physics at the bottom quark scale can be written as [80, 81]

$$C_{7,NP}(\mu_b) \approx 0.5696C_{7,NP}(\mu_{EW}) + 0.1107C_{8,NP}(\mu_{EW}), \quad (28)$$

where

$$\begin{aligned} C_{7,NP}(\mu_{EW}) &= C_{7,NP}^{(a)}(\mu_{EW}) + C_{7,NP}^{(b)}(\mu_{EW}) + C_{7,NP}^{(c)}(\mu_{EW}) + C_{7,NP}^{(d)}(\mu_{EW}) + \\ &C_{7,NP}^{\prime(a)}(\mu_{EW}) + C_{7,NP}^{\prime(b)}(\mu_{EW}) + C_{7,NP}^{\prime(c)}(\mu_{EW}) + C_{7,NP}^{\prime(d)}(\mu_{EW}) + \\ &C_{7,NP}^{WW}(\mu_{EW}) + C_{7,NP}^{WH}(\mu_{EW}), \\ C_{8,NP}(\mu_{EW}) &= C_{8g,NP}(\mu_{EW}) + C_{8g,NP}'(\mu_{EW}) + C_{8,NP}^{WW}(\mu_{EW}) + C_{8,NP}^{WH}(\mu_{EW}). \end{aligned} \quad (29)$$

IV. RARE DECAY $B_s^0 \rightarrow \mu^+ \mu^-$

Fig. 3 shows the main one loop vertex and box diagrams contributing to the process $B_s^0 \rightarrow \mu^+ \mu^-$ in the TNMSSM. In Fig. 3, newly defined up-squarks and pseudo-scalar Higgs bosons will make new contributions to the branching ratio $\text{Br}(B_s^0 \rightarrow \mu^+ \mu^-)$ compared to the MSSM. Considering Fig. 2 and Fig. 3, the Wilson coefficients corresponding to the process $B_s^0 \rightarrow \mu^+ \mu^-$ at the EW scale can be written as

$$\begin{aligned} C_{S,NP}(\mu_{EW}) &= \frac{\sqrt{2}s_W c_W}{4m_b e^3 V_{ts}^* V_{tb}} \left[C_{S,NP}^{(1)}(\mu_{EW}) + C_{S,NP}^{(2)}(\mu_{EW}) + C_{S,NP}^{(3)}(\mu_{EW}) + C_{S,NP}^{(4)}(\mu_{EW}) \right. \\ &\quad \left. + C_{S,NP}^{(6)}(\mu_{EW}) + C_{S,NP}^{(9)}(\mu_{EW}) + C_{S,NP}^{(11)}(\mu_{EW}) \right], \\ C_{S,NP}'(\mu_{EW}) &= C_{S,NP}(\mu_{EW})(L \leftrightarrow R), \\ C_{P,NP}(\mu_{EW}) &= \frac{\sqrt{2}s_W c_W}{4m_b e^3 V_{ts}^* V_{tb}} \left[C_{P,NP}^{(1)}(\mu_{EW}) + C_{P,NP}^{(2)}(\mu_{EW}) + C_{P,NP}^{(3)}(\mu_{EW}) + C_{P,NP}^{(4)}(\mu_{EW}) \right. \\ &\quad \left. + C_{P,NP}^{(6)}(\mu_{EW}) + C_{P,NP}^{(9)}(\mu_{EW}) + C_{P,NP}^{(11)}(\mu_{EW}) \right], \\ C_{P,NP}'(\mu_{EW}) &= -C_{P,NP}(\mu_{EW})(L \leftrightarrow R), \\ C_{9,NP}(\mu_{EW}) &= \frac{\sqrt{2}s_W c_W g_s^2}{64\pi^2 e^3 V_{ts}^* V_{tb}} \left[C_{9,NP}^{(5)}(\mu_{EW}) + C_{9,NP}^{(6)}(\mu_{EW}) + C_{9,NP}^{(7)}(\mu_{EW}) + C_{9,NP}^{(8)}(\mu_{EW}) \right. \\ &\quad \left. + C_{9,NP}^{(9)}(\mu_{EW}) + C_{9,NP}^{(10)}(\mu_{EW}) + C_{9,NP}^{WW}(\mu_{EW}) \right], \\ C_{9,NP}'(\mu_{EW}) &= C_{9,NP}(\mu_{EW})(L \leftrightarrow R), \end{aligned}$$

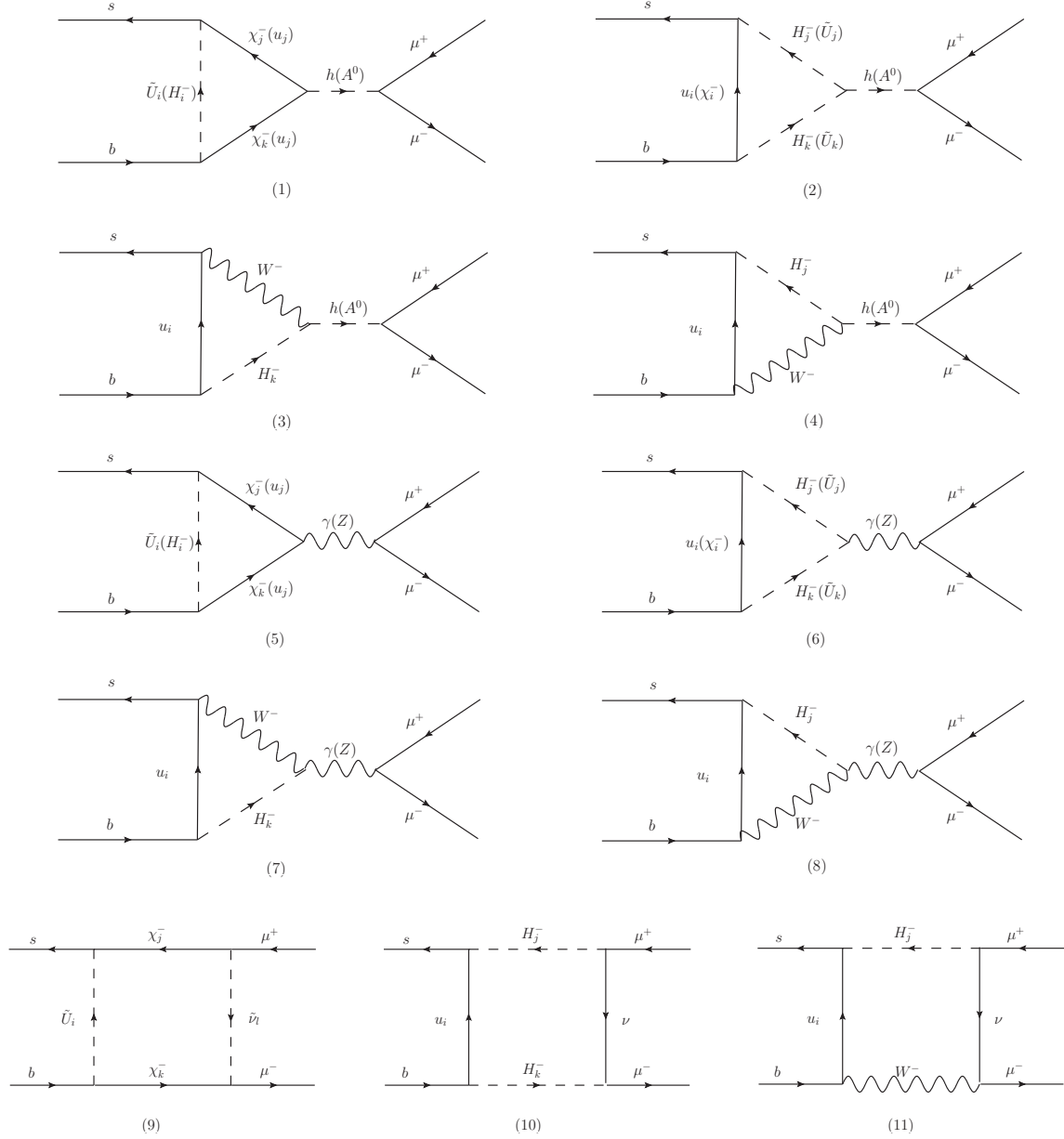


FIG. 3: The one loop vertex and box diagrams contributing to $B_s^0 \rightarrow \mu^+ \mu^-$ in the TNMSSM.

$$\begin{aligned}
C_{10,NP}(\mu_{EW}) &= \frac{\sqrt{2}s_W c_W g_s^2}{64\pi^2 e^3 V_{ts}^* V_{tb}} \left[C_{10,NP}^{(5)}(\mu_{EW}) + C_{10,NP}^{(6)}(\mu_{EW}) + C_{10,NP}^{(7)}(\mu_{EW}) + C_{10,NP}^{(8)}(\mu_{EW}) \right. \\
&\quad \left. + C_{10,NP}^{(9)}(\mu_{EW}) + C_{10,NP}^{(10)}(\mu_{EW}) + C_{10,NP}^{WW}(\mu_{EW}) \right], \\
C'_{10,NP}(\mu_{EW}) &= -C_{10,NP}(\mu_{EW})(L \leftrightarrow R).
\end{aligned} \tag{30}$$

$C_7^{eff,SM}$	$C_8^{eff,SM}$	$C_9^{eff,SM} - Y(q^2)$	$C_{10}^{eff,SM}$
-0.304	-0.167	4.211	-4.103

TABLE I: At hadronic scale $\mu = m_b \simeq 4.65\text{GeV}$, Wilson coefficients from the SM to NNLL accuracy.

All of the Wilson coefficients calculated above are gauge invariant and the concrete expressions on the right side of Eq.(30) are collected in Appendix B. In addition, the Wilson coefficients can also be evolved from EW scale μ_{EW} down to hadronic scale $\mu \sim m_b$ by the renormalization group equations. For obtaining hadronic matrix elements conveniently, we define effective coefficients as [72]

$$\begin{aligned}
C_7^{eff} &= \frac{4\pi}{\alpha_s} C_7 - \frac{1}{3} C_3 - \frac{4}{9} C_4 - \frac{20}{3} C_5 - \frac{80}{9} C_6, \\
C_8^{eff} &= \frac{4\pi}{\alpha_s} C_8 + C_3 - \frac{1}{6} C_4 + 20 C_5 - \frac{10}{3} C_6, \\
C_9^{eff} &= \frac{4\pi}{\alpha_s} C_9 + Y(q^2), \quad C_{10}^{eff} = \frac{4\pi}{\alpha_s} C_{10}, \\
C'_{7,8,9,10}{}^{eff} &= \frac{4\pi}{\alpha_s} C'_{7,8,9,10}.
\end{aligned} \tag{31}$$

The Wilson coefficients at hadronic energy scale from the SM to Next-to-Next-to-Logarithmic (NNLL) accuracy are shown in Table I. And the renormalization group equations are written as

$$\begin{aligned}
\vec{C}_{NP}(\mu) &= \hat{U}(\mu, \mu_0) \vec{C}_{NP}(\mu_0), \\
\vec{C}'_{NP}(\mu) &= \hat{U}'(\mu, \mu_0) \vec{C}'_{NP}(\mu_0)
\end{aligned} \tag{32}$$

with

$$\begin{aligned}
\vec{C}_{NP}^T &= (C_{1,NP}, \dots, C_{6,NP}, C_{7,NP}^{eff}, C_{8,NP}^{eff}, C_{9,NP}^{eff} - Y(q^2), C_{10,NP}^{eff}), \\
\vec{C}'_{NP}{}^T &= (C'_{7,NP}{}^{eff}, C'_{8,NP}{}^{eff}, C'_{9,NP}{}^{eff}, C'_{10,NP}{}^{eff}),
\end{aligned} \tag{33}$$

and

$$\hat{U}(\mu, \mu_0) \simeq 1 - \left[\frac{1}{2\beta_0} \ln \frac{\alpha_s(\mu)}{\alpha_s(\mu_0)} \right] \hat{\gamma}^{(0)T},$$

$$\widehat{U}(\mu, \mu_0) \simeq 1 - \left[\frac{1}{2\beta_0} \ln \frac{\alpha_s(\mu)}{\alpha_s(\mu_0)} \right] \widehat{\gamma}'^{(0)T}, \quad (34)$$

where Ref. [82] provided the anomalous dimension matrices as

$$\widehat{\gamma}^{(0)} = \begin{pmatrix} -4 & \frac{8}{3} & 0 & -\frac{2}{9} & 0 & 0 & -\frac{208}{243} & \frac{173}{162} & -\frac{2272}{729} & 0 \\ 12 & 0 & 0 & \frac{4}{3} & 0 & 0 & \frac{416}{81} & \frac{70}{27} & \frac{1952}{243} & 0 \\ 0 & 0 & 0 & -\frac{52}{3} & 0 & 2 & -\frac{176}{81} & \frac{14}{27} & -\frac{6752}{243} & 0 \\ 0 & 0 & -\frac{40}{9} & -\frac{100}{9} & \frac{4}{9} & \frac{5}{6} & -\frac{152}{243} & -\frac{587}{162} & -\frac{2192}{729} & 0 \\ 0 & 0 & 0 & -\frac{256}{3} & 0 & 20 & -\frac{6272}{81} & \frac{6596}{27} & -\frac{84032}{243} & 0 \\ 0 & 0 & -\frac{256}{9} & \frac{56}{9} & \frac{40}{9} & -\frac{2}{3} & \frac{4624}{243} & \frac{4772}{81} & -\frac{37856}{729} & 0 \\ 0 & 0 & 0 & 0 & 0 & 0 & \frac{32}{3} & 0 & 0 & 0 \\ 0 & 0 & 0 & 0 & 0 & 0 & -\frac{32}{9} & \frac{28}{3} & 0 & 0 \\ 0 & 0 & 0 & 0 & 0 & 0 & 0 & 0 & 0 & 0 \\ 0 & 0 & 0 & 0 & 0 & 0 & 0 & 0 & 0 & 0 \end{pmatrix},$$

$$\widehat{\gamma}'^{(0)} = \begin{pmatrix} \frac{32}{3} & 0 & 0 & 0 \\ -\frac{32}{9} & \frac{28}{3} & 0 & 0 \\ 0 & 0 & 0 & 0 \\ 0 & 0 & 0 & 0 \end{pmatrix}. \quad (35)$$

Based on the Wilson coefficients above, the branching ratio of $B_s^0 \rightarrow \mu^+ \mu^-$ can be given by

$$\text{Br}(B_s^0 \rightarrow \mu^+ \mu^-) = \frac{\tau_{B_s^0}}{16\pi} \frac{|\mathcal{M}_s|^2}{M_{B_s^0}^2} \sqrt{1 - \frac{4m_\mu^2}{M_{B_s^0}^2}}, \quad (36)$$

where $M_{B_s^0} = 5.367\text{GeV}$ denotes the mass of neutral meson B_s^0 and $\tau_{B_s^0} = 1.466(31)\text{ps}$ denotes its life time. Moreover, the squared amplitude can be written as

$$|\mathcal{M}_s|^2 = 16G_F^2 |V_{tb}V_{ts}^*|^2 M_{B_s^0}^2 \left[|F_S^s|^2 + |F_P^s + 2m_\mu F_A^s|^2 \right], \quad (37)$$

with

$$F_S^s = \frac{\alpha_{EW}(\mu_b)}{8\pi} \frac{m_b M_{B_s^0}^2}{m_b + m_s} f_{B_s^0} (C_S - C'_S), \quad (38)$$

$$F_P^s = \frac{\alpha_{EW}(\mu_b)}{8\pi} \frac{m_b M_{B_s^0}^2}{m_b + m_s} f_{B_s^0} (C_P - C'_P), \quad (39)$$

$$F_A^s = \frac{\alpha_{EW}(\mu_b)}{8\pi} f_{B_s^0} \left[C_{10}^{eff}(\mu_b) - C'_{10}{}^{eff}(\mu_b) \right], \quad (40)$$

where $f_{B^0} = (227 \pm 8)\text{MeV}$ denote the decay constants.

V. NUMERICAL ANALYSES

This section provides the numerical discussion of the branching ratios of B meson rare decays $\bar{B} \rightarrow X_s \gamma$ and $B_s^0 \rightarrow \mu^+ \mu^-$ by considering the latest multiple experimental constraints of particles. It includes that the SM-like Higgs mass m_h is kept around 125.25 GeV, the neutralino mass is limited to more than 116 GeV, the chargino mass is limited to more than 1100 GeV, the slepton mass is limited to more than 700 GeV and the squark mass is maintained at the TeV order of magnitude [1, 83–90]. Additionally, the first two generations of squarks are strongly constrained by direct searches at the LHC [91, 92]. However, compared to the previous two generations, the mass of the third generation squark which can affect the mass of SM-like Higgs do not suffer strong constraints. Therefore we take $m_{\tilde{q}} = m_{\tilde{u}} = \text{diag}(2, 2, m_{\tilde{t}})$ TeV, and the discussion about the observed Higgs signal in Ref.[93] limits $m_{\tilde{t}} \gtrsim 1.5$ TeV. For simplicity, we also choose $T_{u_{1,2}} = Y_{u_{1,2}} A_{u_{1,2}}$, $A_{u_{1,2}} = 1$ TeV. As a key parameter, $T_{u_3} = A_t$ affects the SM-like Higgs mass and the numerical calculation obviously. In order to obtain reasonable numerical results, we need to find some sensitive parameters for discussion. Similarly to the MSSM [94], the new physics contributions to the branching ratios $\text{Br}(\bar{B} \rightarrow X_s \gamma)$ and $\text{Br}(B_s^0 \rightarrow \mu^+ \mu^-)$ are also depended on $\tan \beta$, A_t and singly-charged Higgs mass. Moreover, according to their great impacts on singly-charged Higgs mass, neutralino mass and chargino mass, we found three other new parameters κ , λ and T_λ that can affect $\text{Br}(\bar{B} \rightarrow X_s \gamma)$ and $\text{Br}(B_s^0 \rightarrow \mu^+ \mu^-)$ in the TNMSSM. We will plot the relational and scatter diagrams and explore the effects of these parameters on the branching ratios and the allowed ranges between λ , κ and T_λ .

By considering the experimental constraints described above, we adopt the parameters in the following numerical calculation as

$$\begin{aligned} \chi_d = \chi_u = 0.1, \quad \Lambda_T = 0.6, \quad \tan \beta' = 5, \quad M_1 = 1 \text{ TeV}, \quad m_{\tilde{t}} = 1.6 \text{ TeV}, \\ M_2 = \mu = 1.2 \text{ TeV}, \quad T_{\chi_d} = T_{\chi_u} = -500 \text{ GeV}, \quad T_\kappa = -300 \text{ GeV}, \quad T_{\Lambda_T} = 100 \text{ GeV}. \end{aligned} \quad (41)$$

To illustrate the effects of A_t and $\tan \beta$ on the branching ratios, we take $\lambda = 0.4$, $\kappa =$

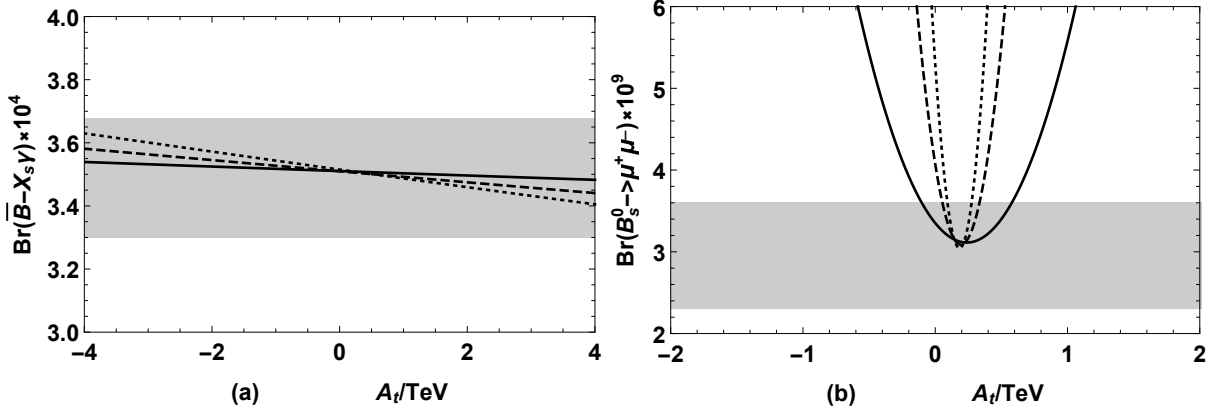


FIG. 4: (a) $\text{Br}(\bar{B} \rightarrow X_s \gamma)$ and (b) $\text{Br}(B_s^0 \rightarrow \mu^+ \mu^-)$ versus A_t for $\tan \beta = 10$ (solid line), $\tan \beta = 25$ (dashed line), $\tan \beta = 40$ (dotted line), where the gray area denotes the experimental 1σ interval.

0.6, $T_\lambda = 100$ GeV and plot the graph of $\text{Br}(\bar{B} \rightarrow X_s \gamma)$ and $\text{Br}(B_s^0 \rightarrow \mu^+ \mu^-)$ varying with A_t in Fig. 4 for $\tan \beta = 10$ (solid line), $\tan \beta = 25$ (dashed line), $\tan \beta = 40$ (dotted line). The gray area denotes the experimental 1σ bounds in Eq.(1). Fig. 4(a) shows that $\text{Br}(\bar{B} \rightarrow X_s \gamma)$ decreases with the increasing of A_t and the slope of evolution is steeper as $\tan \beta$ is bigger. In Fig. 4(b), we can see that the variation relationship between A_t and $\text{Br}(B_s^0 \rightarrow \mu^+ \mu^-)$ is almost the shape of parabolic. Moreover, when $\tan \beta$ is bigger, A_t is limited strongly in the smaller range by the experimental data on $\text{Br}(B_s^0 \rightarrow \mu^+ \mu^-)$. It will be seen from this that the new physics can provide the considerable contributions to $\text{Br}(B_s^0 \rightarrow \mu^+ \mu^-)$ for large $\tan \beta$ and A_t .

To see the effects of λ , κ , and T_λ on the branching ratios, we first take $\lambda = 0.4$, $\tan \beta = 5$, $A_t = 0.5$ TeV and plot the graph of $\text{Br}(\bar{B} \rightarrow X_s \gamma)$ and $\text{Br}(B_s^0 \rightarrow \mu^+ \mu^-)$ varying with T_λ in Fig. 5, for $\kappa = 0.4$ (solid line), $\kappa = 0.5$ (dashed line), $\kappa = 0.6$ (dotted line), respectively. Then, we take $T_\lambda = 100$ GeV, $\tan \beta = 5$, $A_t = 0.5$ TeV and plot the graph of $\text{Br}(\bar{B} \rightarrow X_s \gamma)$ and $\text{Br}(B_s^0 \rightarrow \mu^+ \mu^-)$ varying with κ in Fig. 6, for $\lambda = 0.9$ (solid line), $\lambda = 0.7$ (dashed line), $\lambda = 0.5$ (dotted line), respectively. The gray area denotes the experimental 1σ bounds. Fig. 5 shows that $\text{Br}(\bar{B} \rightarrow X_s \gamma)$ and $\text{Br}(B_s^0 \rightarrow \mu^+ \mu^-)$ increase with the decreasing of T_λ when T_λ is negative and the three lines mix together for large T_λ . Thus it

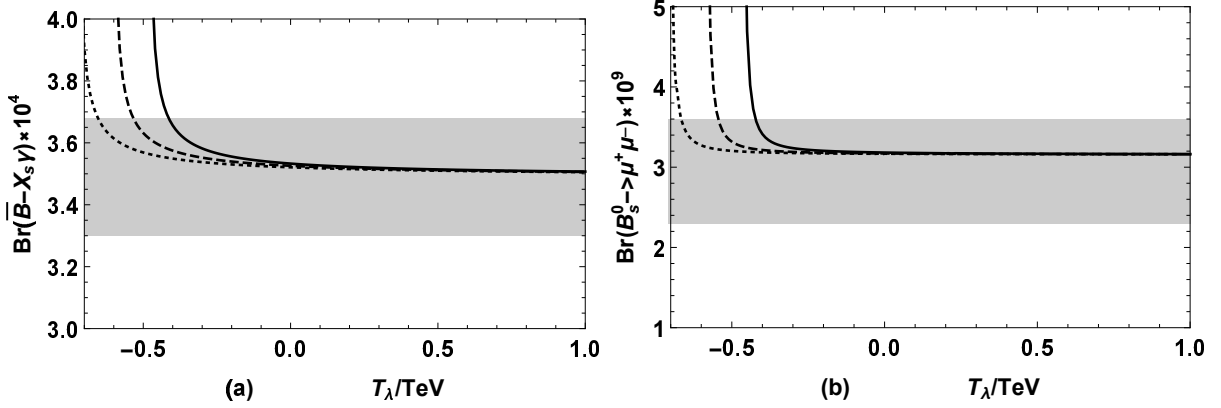


FIG. 5: (a) $\text{Br}(\bar{B} \rightarrow X_s \gamma)$ and (b) $\text{Br}(B_s^0 \rightarrow \mu^+ \mu^-)$ versus T_λ for $\kappa = 0.4$ (solid line), $\kappa = 0.5$ (dashed line), $\kappa = 0.6$ (dotted line) when $\lambda = 0.4$. The gray area denotes the experimental 1σ interval.

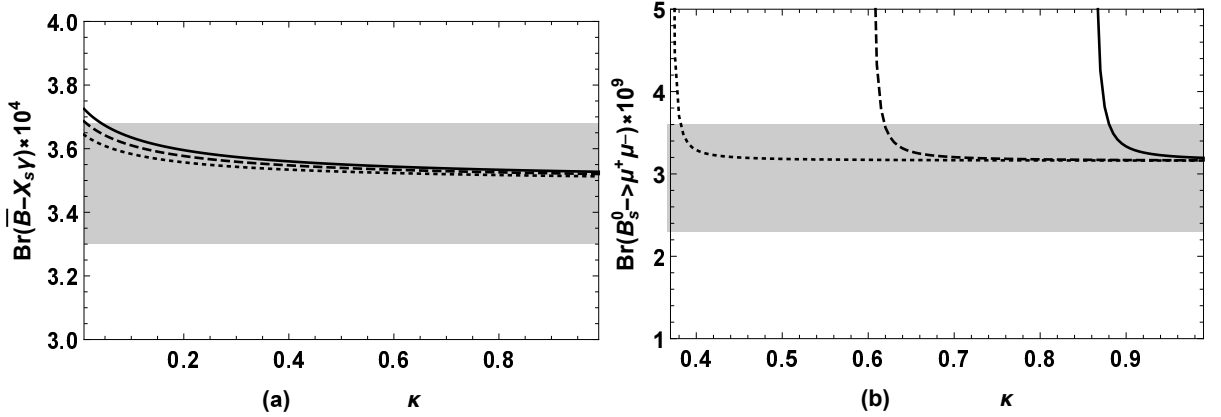


FIG. 6: (a) $\text{Br}(\bar{B} \rightarrow X_s \gamma)$ and (b) $\text{Br}(B_s^0 \rightarrow \mu^+ \mu^-)$ versus κ for $\lambda = 0.9$ (solid line), $\lambda = 0.7$ (dashed line), $\lambda = 0.5$ (dotted line) when $T_\lambda = 100$ GeV. The gray area denotes the experimental 1σ interval.

can be seen that the smaller κ is taken, the smaller range of T_λ is limited and large T_λ can get rid of the influence of κ . In Fig. 6(a), $\text{Br}(\bar{B} \rightarrow X_s \gamma)$ decreases gradually with the increasing of κ and κ is less affected by λ . However, from Fig. 6(b), $\text{Br}(B_s^0 \rightarrow \mu^+ \mu^-)$ decreases dramatically near $\kappa = 0.4$ for $\lambda = 0.5$, $\kappa = 0.6$ for $\lambda = 0.7$ and $\kappa = 0.9$ for $\lambda = 0.9$ respectively. It indicates that λ has strong limitations on κ and the limitations will be discussed in the

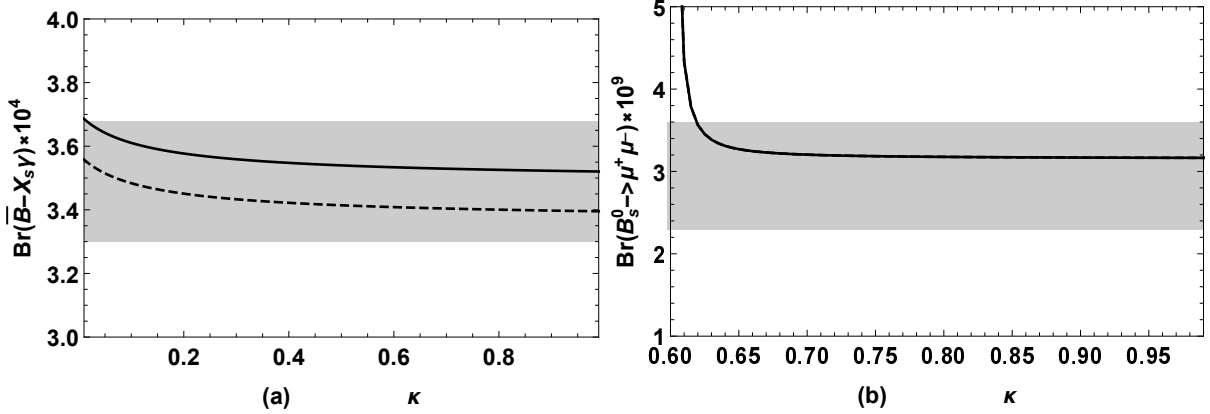


FIG. 7: The comparison graph of two loop (solid lines) result and one loop (dashed lines) result when $\lambda = 0.7$, $T_\lambda = 100$ GeV, where the gray area denotes the experimental 1σ interval.

following by drawing scatter plots.

Meanwhile, for comparing and reflecting the specific differences between one loop and two loop corrections to $\bar{B} \rightarrow X_s \gamma$ and $B_s^0 \rightarrow \mu^+ \mu^-$, we take $T_\lambda = 100$ GeV, $\lambda = 0.7$ and plot the graph of $\text{Br}(\bar{B} \rightarrow X_s \gamma)$ and $\text{Br}(B_s^0 \rightarrow \mu^+ \mu^-)$ varying with κ in Fig. 7. The solid and dashed line denote two loop and one loop predictions respectively. Fig. 7(a) shows that, the relative corrections from two loop diagrams to one loop corrections of $\text{Br}(\bar{B} \rightarrow X_s \gamma)$ can reach around 4%, which can produce a more precise prediction on the process $\bar{B} \rightarrow X_s \gamma$. In Fig. 7(b), we can see that the two lines almost overlap which shows that the two loop corrections are negligible compared with one loop corrections. Therefore, in the analysis of the numerical calculations above, we always use the more precise two loop predictions.

Now, for revealing how λ , κ , and T_λ be constrained by the experimental measurements of B meson rare decays, we scan the sensitive parameters under the consideration of the experimental constraints above and $\text{Br}(\bar{B} \rightarrow X_s \gamma)$, $\text{Br}(B_s^0 \rightarrow \mu^+ \mu^-)$ within one standard deviation. The random ranges of input parameters are as follows:

$$\begin{aligned} \tan \beta &= (1, 40), \quad \lambda = (0.01, 0.99), \quad \kappa = (0.01, 0.99), \\ \mu &= (1.1, 1.5) \text{ TeV}, \quad T_\lambda = (-1, 1) \text{ TeV}, \quad A_t = (-4, 4) \text{ TeV}. \end{aligned} \quad (42)$$

Then, we plot the allowed ranges of κ versus λ , T_λ versus λ and κ versus T_λ in Fig. 8.

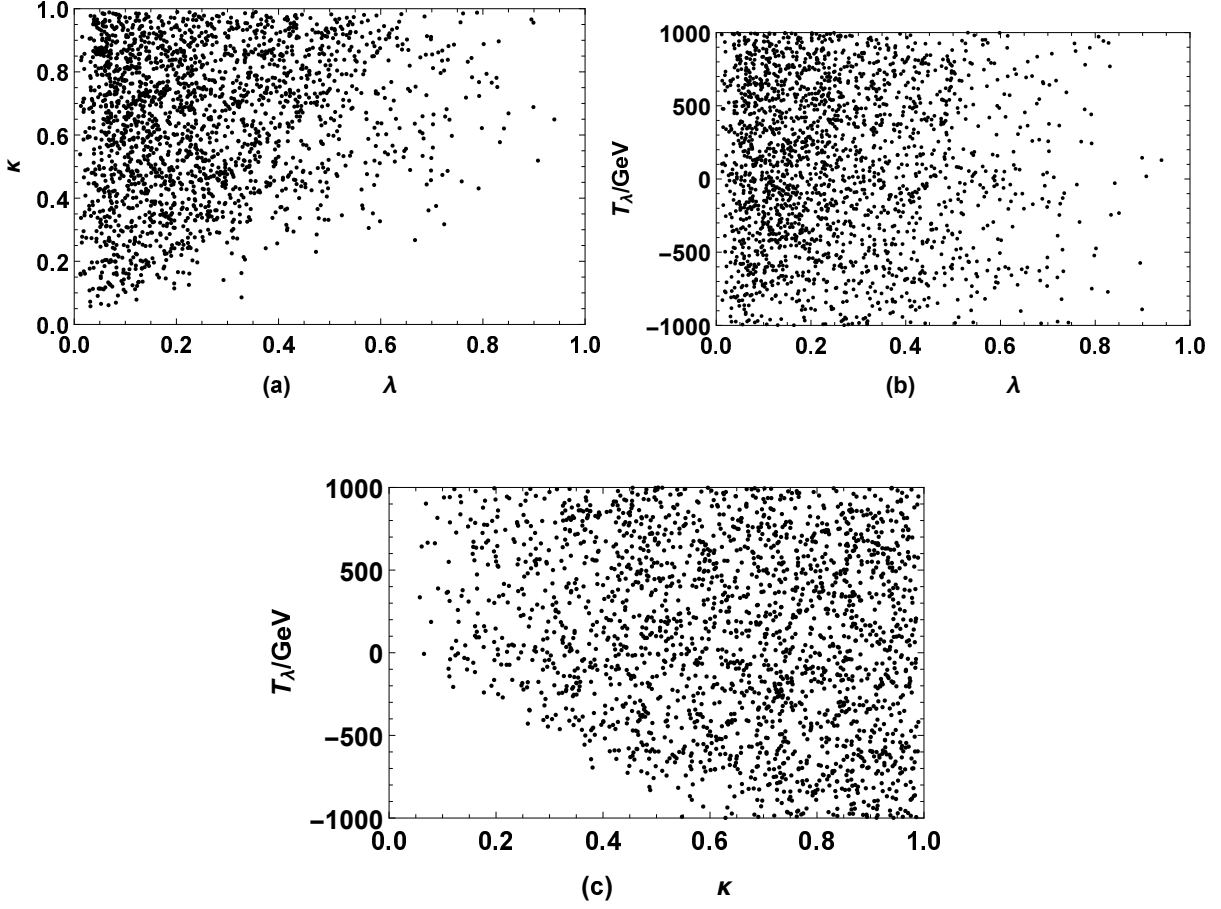


FIG. 8: Scanning the parameter space in Eq.(42) and keeping $\text{Br}(\bar{B} \rightarrow X_s \gamma)$, $\text{Br}(B_s^0 \rightarrow \mu^+ \mu^-)$ in the experimental 1σ interval, the allowed ranges of $\kappa - \lambda$ (a), $T_\lambda - \lambda$ (b), $T_\lambda - \kappa$ (c) are plotted.

Fig. 8(a) shows that the vast majority of points are concentrated in the areas $\kappa > \lambda$ and the number of points gradually decreases as $\kappa < \lambda$. In Fig. 8(b), we can find that the density of points decreases with the increasing of λ and this phenomenon is more obvious when $\lambda > 0.6$. As shown in Fig. 8(c), the negative range of T_λ is gradually limited when $\kappa < 0.6$. In conclusion, maintaining $\text{Br}(\bar{B} \rightarrow X_s \gamma)$ and $\text{Br}(B_s^0 \rightarrow \mu^+ \mu^-)$ within the experimental 1σ interval prefers λ , κ in the range $\lambda < 0.6$, $\kappa > 0.6$ and positive T_λ .

VI. SUMMARY

B meson rare decays are sensitive to the searching on new physics beyond the SM. In this paper, we investigate the two loop electroweak corrections to the processes $\bar{B} \rightarrow X_s \gamma$ and $B_s^0 \rightarrow \mu^+ \mu^-$ in the TNMSSM which extends the MSSM with two triplets and one singlet. Under the consideration of the constraints from the observed Higgs signal and the updated experimental data of the branching ratios, the numerical results indicate that the corrections from two loop diagrams to the process $\bar{B} \rightarrow X_s \gamma$ in the TNMSSM can reach around 4%, which can produce a more precise theoretical prediction. Moreover, the new physics effects in the TNMSSM can fit the experimental data for the rare decays $\bar{B} \rightarrow X_s \gamma$ and $B_s^0 \rightarrow \mu^+ \mu^-$, and the corresponding parameter space is limited strictly by considering $\text{Br}(\bar{B} \rightarrow X_s \gamma)$ and $\text{Br}(B_s^0 \rightarrow \mu^+ \mu^-)$ in the experimental 1σ intervals. The new parameters λ , κ , T_λ in the TNMSSM have great impacts on the theoretical predictions of $\text{Br}(\bar{B} \rightarrow X_s \gamma)$, $\text{Br}(B_s^0 \rightarrow \mu^+ \mu^-)$ and maintaining $\text{Br}(\bar{B} \rightarrow X_s \gamma)$ and $\text{Br}(B_s^0 \rightarrow \mu^+ \mu^-)$ within the experimental 1σ interval prefers λ , κ in the range $\lambda < 0.6$, $\kappa > 0.6$ and positive T_λ .

Acknowledgments

Our deepest gratitude goes to professor Tai-Fu Feng for his sincere guidance on this research. The work has been supported by the National Natural Science Foundation of China (NNSFC) with Grants No. 12075074, No. 12235008, No. 11535002, No. 11705045, Hebei Natural Science Foundation for Distinguished Young Scholars with Grant No. A2022201017, Natural Science Foundation of Guangxi Autonomous Region with Grant No. 2022GXNSFDA035068, and the youth top-notch talent support program of the Hebei Province.

Appendix A: The corresponding matrix elements

The matrix elements of the squared mass matrix for singly-charged Higgs can be given by

$$\begin{aligned}
m_{H_d^- H_d^-,*} &= \frac{\sqrt{2}}{2} T_\lambda \tan \beta v_S - \sqrt{2} T_{\chi_d} v_T + \frac{1}{4} g_2^2 (\tan^2 \beta v_d^2 + 2v_T^2 - 2v_{\bar{T}}^2) - \frac{1}{2} \lambda^2 \tan^2 \beta v_d^2 \\
&\quad + \Lambda_T \chi_d v_S v_{\bar{T}} - 2\chi_d^2 v_T^2 + \frac{1}{2} \lambda \tan \beta (\kappa v_S^2 - \Lambda_T v_T v_{\bar{T}} + 2v_S (\chi_d v_T + \chi_u v_{\bar{T}})), \\
m_{H_u^+,* H_u^+} &= \frac{1}{4 \tan \beta} (2\sqrt{2} T_\lambda v_S + g_2^2 \tan \beta (v_d^2 - 2v_T^2 + 2v_{\bar{T}}^2) - 2 \tan \beta (2\sqrt{2} T_{\chi_u} v_{\bar{T}} + \lambda^2 v_d^2 \\
&\quad - 2\Lambda_T \chi_u v_S v_T + 4\chi_u^2 v_{\bar{T}}^2) + 2\lambda (\kappa v_S^2 - \Lambda_T v_T v_{\bar{T}} + 2(\chi_d v_T + \chi_u v_{\bar{T}}) v_S)), \\
m_{\bar{T}^- \bar{T}^-,*} &= \frac{1}{4} (2\sqrt{2} T_{\Lambda_T} \tan \beta' v_S - g_2^2 v_d^2 + 2g_2^2 v_T^2 + 2\kappa \Lambda_T \tan \beta' v_S^2 - 2\Lambda_T^2 v_T^2 + \frac{2\Lambda_T \chi_d v_d^2 v_S}{v_{\bar{T}}} \\
&\quad - 2 \tan \beta \lambda v_d^2 (\Lambda_T \tan \beta' - \frac{2\chi_u v_S}{v_{\bar{T}}}) + \tan^2 \beta v_d^2 (-\frac{2\sqrt{2} T_{\chi_u}}{v_{\bar{T}}} + g_2^2 - 4\chi_u^2)), \\
m_{T^+,* T^+} &= \frac{1}{4} (-\frac{2\sqrt{2} T_{\chi_d} v_d^2}{v_T} + g_2^2 (v_d^2 - \tan^2 \beta v_d^2 + 2v_{\bar{T}}^2) + 2(\frac{\sqrt{2} T_{\Lambda_T} v_S}{\tan \beta'} \\
&\quad + \frac{\kappa \Lambda_T v_S^2}{\tan \beta'} - \frac{\lambda \Lambda_T \tan \beta v_d^2}{\tan \beta'} - \Lambda_T^2 v_T^2 - 2\chi_d^2 v_d^2 + \frac{\tan \beta v_d^2 v_S}{v_T} (2\lambda \chi_d + \tan \beta \Lambda_T \chi_u))), \\
m_{H_u^+,* H_d^-,*} &= m_{H_d^- H_u^+} = \frac{1}{4} (g_2^2 \tan \beta v_d^2 + 2\sqrt{2} T_\lambda v_S - 2\lambda (-\kappa v_S^2 + \lambda \tan \beta v_d^2 + \Lambda_T v_T v_{\bar{T}})), \\
m_{\bar{T}^- H_d^-,*} &= m_{H_d^- \bar{T}^-,*} = \frac{1}{2\sqrt{2}} v_d (g_2^2 v_{\bar{T}} - 2(\Lambda_T \chi_d + \lambda \chi_u \tan \beta) v_S), \\
m_{T^+,* H_d^-,*} &= m_{H_d^- T^+} = \frac{1}{4} v_d (-4T_{\chi_d} + \sqrt{2} (g_2^2 v_T + 2\chi_d (\lambda \tan \beta v_S - 2\chi_d v_T))), \\
m_{\bar{T}^- H_u^+,*} &= m_{H_u^+ \bar{T}^-,*} = \frac{1}{4} v_d (-4 \tan \beta T_{\chi_u} + 2\sqrt{2} \lambda \chi_u v_S + \sqrt{2} \tan \beta v_{\bar{T}} (g_2^2 - 4\chi_u^2)), \\
m_{T^+,* H_u^+} &= m_{H_u^+ T^+} = \frac{v_d}{2\sqrt{2}} (g_2^2 \tan \beta v_T - 2v_S (\lambda \chi_d + \tan \beta \Lambda_T \chi_u)), \\
m_{T^+,* \bar{T}^-,*} &= m_{\bar{T}^- T^+} = \frac{1}{2} (\sqrt{2} T_{\Lambda_T} v_S + g_2^2 v_T v_{\bar{T}} - \Lambda_T (-\kappa v_S^2 + \lambda \tan \beta v_d^2 + \Lambda_T v_T v_{\bar{T}})), \quad (\text{A1})
\end{aligned}$$

where $\tan \beta = \frac{v_u}{v_d}$ and $\tan \beta' = \frac{v_T}{v_{\bar{T}}}$.

The matrix elements of the squared mass matrix for CP-even Higgs are written as

$$\begin{aligned}
m_{H_d^0 H_d^0} &= \frac{1}{4} ((g^2 + 8\chi_d^2) v_d^2 + 2 \tan \beta v_S N - 2\lambda \Lambda_T \tan \beta \tan \beta' v_T^2), \\
m_{H_u^0 H_u^0} &= \frac{1}{4} ((g^2 + 8\chi_u^2) v_d^2 + \frac{2v_S}{\tan \beta} N - 2\lambda \Lambda_T \frac{\tan \beta'}{\tan \beta} v_T^2), \\
m_{H_u^0 H_d^0} &= \frac{1}{4} ((-g^2 + 4\lambda^2) \tan \beta v_d^2 - 2v_S N + 2\lambda \Lambda_T \tan \beta' v_T^2),
\end{aligned}$$

$$\begin{aligned}
m_{SS} &= \frac{1}{2} \left(\frac{\tan \beta v_d^2}{v_S} (x + \sqrt{2} T_\lambda + 2n) + \frac{1}{v_S} (\Lambda_T \chi_d v_d^2 v_{\bar{T}} + \sqrt{2} T_{\Lambda_T} \tan \beta' v_{\bar{T}}^2) \right. \\
&\quad \left. + \sqrt{2} T_\kappa v_S + 4\kappa^2 v_S^2 \right), \\
m_{SH_d^0} &= \frac{-1}{2} v_d (\sqrt{2} \tan \beta T_\lambda - 2\lambda^2 v_S + 2 \tan \beta n + 2 \tan \beta \lambda \kappa v_S + 2 \Lambda_T \chi_d v_{\bar{T}}), \\
m_{SH_u^0} &= -\frac{T_\lambda v_d}{\sqrt{2}} - v_d (\lambda v_S (\kappa - \lambda \tan \beta) + n + x), \\
m_{T^0 T^0} &= g^2 \tan^2 \beta' v_{\bar{T}}^2 + \frac{1}{2 \tan \beta' v_{\bar{T}}} (\sqrt{2} T_{\Lambda_T} v_S v_{\bar{T}} - \sqrt{2} T_{\chi_d} v_d^2 + \kappa \Lambda_T v_S^2 v_{\bar{T}} \\
&\quad + \tan \beta v_d^2 (2\lambda \chi_d v_S + \tan \beta \Lambda_T \chi_u v_S - \lambda \Lambda_T v_{\bar{T}})), \\
m_{H_d^0 T^0} &= \frac{v_d}{2} (2\sqrt{2} T_{\chi_d} - g^2 \tan \beta' v_{\bar{T}} + \lambda \tan \beta (\Lambda_T v_{\bar{T}} - 2\chi_d v_S) + 8 \tan \beta' \chi_d^2 v_{\bar{T}}), \\
m_{H_u^0 T^0} &= \frac{v_d}{2} (g^2 \tan \beta \tan \beta' v_{\bar{T}} + \lambda \Lambda_T v_{\bar{T}} - 2\lambda \chi_d v_S - 2 \tan \beta \Lambda_T \chi_u v_S), \\
m_{ST^0} &= -\frac{T_{\Lambda_T} v_{\bar{T}}}{\sqrt{2}} + \Lambda_T v_S v_{\bar{T}} (-\kappa + \tan \beta' \Lambda_T) - \frac{1}{2} \tan \beta v_d^2 (2\lambda \chi_d + \tan \beta \Lambda_T \chi_u), \\
m_{\bar{T}^0 \bar{T}^0} &= g^2 v_{\bar{T}}^2 + \frac{1}{2} \tan \beta' v_S (\sqrt{2} T_{\Lambda_T} + \kappa \Lambda_T v_S) + \frac{1}{2 v_{\bar{T}}} (-\sqrt{2} \tan^2 \beta T_{\chi_u} v_d^2 \\
&\quad + \Lambda_T \chi_d v_d^2 v_S + \lambda \tan \beta v_d^2 (-\tan \beta' \Lambda_T v_{\bar{T}} + 2\chi_u v_S)), \\
m_{H_d^0 \bar{T}^0} &= \frac{1}{2} v_d (g^2 v_{\bar{T}} + \lambda \Lambda_T \tan \beta \tan \beta' v_{\bar{T}} - 2\Lambda_T \chi_d v_S - 2\lambda \chi_u \tan \beta v_S), \\
m_{H_u^0 \bar{T}^0} &= \frac{1}{2} v_d (2\sqrt{2} \tan \beta T_{\chi_u} + \lambda (\Lambda_T \tan \beta v_{\bar{T}} - 2\chi_u v_S) - \tan \beta v_{\bar{T}} (g^2 - 8\chi_u^2)), \\
m_{S\bar{T}^0} &= \Lambda_T^2 v_S v_{\bar{T}} - \frac{1}{2} \tan \beta' v_{\bar{T}} (\sqrt{2} T_{\Lambda_T} + 2\kappa \Lambda_T v_S) - \frac{1}{2} v_d^2 (\Lambda_T \chi_d + 2 \tan \beta \lambda \chi_u), \\
m_{T^0 \bar{T}^0} &= \frac{1}{2} (-\sqrt{2} T_{\Lambda_T} v_S - 2g^2 \tan \beta' v_{\bar{T}}^2 - \kappa \Lambda_T v_S^2 + \lambda \Lambda_T \tan \beta v_d^2 + 2 \tan \beta' \Lambda_T^2 v_{\bar{T}}^2), \quad (\text{A2})
\end{aligned}$$

where $g^2 = g_1^2 + g_2^2$, $N = \sqrt{2} T_\lambda + \kappa \lambda v_S + 2\lambda \chi_d \tan \beta' v_{\bar{T}} + 2\lambda \chi_u v_{\bar{T}}$, $x = \Lambda_T \chi_u \tan \beta \tan \beta' v_{\bar{T}}$, $n = \lambda v_{\bar{T}} (\tan \beta' \chi_d + \chi_u)$.

Appendix B: The corresponding Wilson coefficients

The one loop Wilson coefficients for the process $\bar{B} \rightarrow X_s \gamma$ are written as

$$\begin{aligned}
C_{7,NP}^{(a)}(\mu_{EW}) &= \sum_{H_i^-, u_j} \frac{s_W^2}{2e^2 V_{ts}^* V_{tb}} \left\{ \frac{1}{2} C_{H_i^- \bar{s} u_j}^R C_{H_i^- \bar{b} u_j}^L [-I_3(x_{u_j}, x_{H_i^-}) + I_4(x_{u_j}, x_{H_i^-})] + \right. \\
&\quad \left. \frac{m_{u_j}}{m_b} C_{H_i^- \bar{s} u_j}^L C_{H_i^- \bar{b} u_j}^L [-I_1(x_{u_j}, x_{H_i^-}) + I_3(x_{u_j}, x_{H_i^-})] \right\}, \quad (\text{B1})
\end{aligned}$$

$$\begin{aligned}
C_{7,NP}^{(b)}(\mu_{EW}) = & \sum_{H_j^-, u_i} \frac{s_W^2}{3e^2 V_{ts}^* V_{tb}} \left\{ \frac{1}{2} C_{H_j^- \bar{s} u_i}^R C_{H_j^- b \bar{u}_i}^L [-I_1(x_{u_i}, x_{H_j^-}) + 2I_3(x_{u_i}, x_{H_j^-}) \right. \\
& - I_4(x_{u_i}, x_{H_j^-})] + \frac{m_{u_i}}{m_b} C_{H_j^- \bar{s} u_i}^L C_{H_j^- b \bar{u}_i}^L [I_1(x_{u_i}, x_{H_j^-}) - I_2(x_{u_i}, x_{H_j^-}) \\
& \left. - I_3(x_{u_i}, x_{H_j^-})] \right\}, \tag{B2}
\end{aligned}$$

$$\begin{aligned}
C_{7,NP}^{(c)}(\mu_{EW}) = & \sum_{U_i^+, \chi_j^-} \frac{s_W^2}{3e^2 V_{ts}^* V_{tb}} \left\{ \frac{1}{2} C_{U_i^+ \bar{s} \chi_j^-}^R C_{U_i^+ b \bar{\chi}_j^-}^L [-I_3(x_{\chi_j^-}, x_{U_i^+}) + I_4(x_{\chi_j^-}, x_{U_i^+})] + \right. \\
& \left. \frac{m_{\chi_j^-}}{m_b} C_{U_i^+ \bar{s} \chi_j^-}^L C_{U_i^+ b \bar{\chi}_j^-}^L [-I_1(x_{\chi_j^-}, x_{U_i^+}) + I_3(x_{\chi_j^-}, x_{U_i^+})] \right\}, \tag{B3}
\end{aligned}$$

$$\begin{aligned}
C_{7,NP}^{(d)}(\mu_{EW}) = & \sum_{U_j^+, \chi_i^-} \frac{s_W^2}{2e^2 V_{ts}^* V_{tb}} \left\{ \frac{1}{2} C_{U_i^+ \bar{s} \chi_i^-}^R C_{U_j^+ b \bar{\chi}_i^-}^L [-I_1(x_{\chi_i^-}, x_{U_j^+}) + 2I_2(x_{\chi_i^-}, x_{U_j^+}) \right. \\
& - I_4(x_{\chi_i^-}, x_{U_j^+})] + \frac{m_{\chi_i^-}}{m_b} C_{U_j^+ \bar{s} \chi_i^-}^L C_{U_j^+ b \bar{\chi}_i^-}^L [I_1(x_{\chi_i^-}, x_{U_j^+}) - I_2(x_{\chi_i^-}, x_{U_j^+}) \\
& \left. - I_3(x_{\chi_i^-}, x_{U_j^+})] \right\}, \tag{B4}
\end{aligned}$$

$$C_{7,NP}^{(\xi)}(\mu_{EW}) = C_{7,NP}'^{(\xi)}(\mu_{EW})(L \leftrightarrow R), \quad (\xi = a, b, c, d), \tag{B5}$$

where $C_{XYZ}^{L,R}$ denote the constant parts of the interaction vertices about particles XYZ , L and R represent the left and right-handed parts respectively.

Denoting $x_i = \frac{m_i^2}{m_W^2}$, the concrete expressions for $I_k (k = 1, \dots, 4)$ can be given as:

$$\begin{aligned}
I_1(x_1, x_2) &= \frac{1 + \ln x_2}{(x_2 - x_1)} + \frac{x_1 \ln x_1 - x_2 \ln x_2}{(x_2 - x_1)^2}, \\
I_2(x_1, x_2) &= -\frac{1 + \ln x_1}{(x_2 - x_1)} - \frac{x_1 \ln x_1 - x_2 \ln x_2}{(x_2 - x_1)^2}, \\
I_3(x_1, x_2) &= \frac{1}{2} \left[\frac{3 + 2 \ln x_2}{(x_2 - x_1)} - \frac{2x_2 + 4x_2 \ln x_2}{(x_2 - x_1)^2} - \frac{2x_1^2 \ln x_1}{(x_2 - x_1)^3} + \frac{2x_2^2 \ln x_2}{(x_2 - x_1)^3} \right], \\
I_4(x_1, x_2) &= \frac{1}{4} \left[\frac{11 + 6 \ln x_2}{(x_2 - x_1)} - \frac{15 + 18x_2 \ln x_2}{(x_2 - x_1)^2} + \frac{6x_2^2 + 18x_2^2 \ln x_2}{(x_2 - x_1)^3} + \right. \\
& \quad \left. \frac{6x_1^3 \ln x_1 - 6x_2^3 \ln x_2}{(x_2 - x_1)^4} \right]. \tag{B6}
\end{aligned}$$

Assuming $m_{\chi_i^\pm}, m_{\chi_j^0} \gg m_W$, the two loop Wilson coefficients for the process $\bar{B} \rightarrow X_s \gamma$ can be given by

$$C_{7,NP}^{WW}(\mu_{EW}) = \sum_{\chi_i^\pm, \chi_j^0} \frac{-1}{8\pi^2} \left\{ (|C_{W^- \bar{\chi}_j^0 \chi_i^+}^L|^2 + |C_{W^- \bar{\chi}_j^0 \chi_i^+}^R|^2) \left[P\left(\frac{1}{8}, \frac{1}{4}, \frac{-1}{48}, \frac{-1}{144}, 1, x_t\right) + \right. \right.$$

$$\begin{aligned}
& \frac{2}{3}P\left(\frac{-11}{12}, \frac{-29}{72}, \frac{-1}{12}, \frac{1}{144}, 1, x_t\right) + (C_{W^-\bar{\chi}_j^0\chi_i^+}^R C_{W^-\bar{\chi}_j^0\chi_i^+}^{L*} + C_{W^-\bar{\chi}_j^0\chi_i^+}^L \\
& C_{W^-\bar{\chi}_j^0\chi_i^+}^{R*})\left[P\left(\frac{1}{16}, \frac{1}{4}, \frac{-1}{16}, \frac{1}{144}, 1, x_t\right) + \frac{2}{3}P\left(\frac{-11}{12}, \frac{-29}{72}, \frac{-1}{12}, \frac{1}{144}, 1, \right. \right. \\
& \left. \left. x_t\right) + \frac{1}{8}(C_{W^-\bar{\chi}_j^0\chi_i^+}^L C_{W^-\bar{\chi}_j^0\chi_i^+}^{R*} - C_{W^-\bar{\chi}_j^0\chi_i^+}^R C_{W^-\bar{\chi}_j^0\chi_i^+}^{L*})\frac{\partial^2 \rho_{2,1}}{\partial x_1^2}(x_W, x_t)\right] \\
& + C_{W^-\bar{\chi}_i^+\chi^{++}}^{L,R} \leftrightarrow C_{W^-\bar{\chi}_j^0\chi_i^+}^{L,R}, \tag{B7}
\end{aligned}$$

$$\begin{aligned}
C_{8,NP}^{WW}(\mu_{EW}) &= \sum_{\chi_i^\pm, \chi_j^0} \frac{-3}{8\pi^2} \left\{ (|C_{W^-\bar{\chi}_j^0\chi_i^+}^L|^2 + |C_{W^-\bar{\chi}_j^0\chi_i^+}^R|^2) P\left(\frac{-11}{12}, \frac{-29}{72}, \frac{-1}{12}, \frac{1}{144}, 1, x_t\right) + \right. \\
& (C_{W^-\bar{\chi}_j^0\chi_i^+}^R C_{W^-\bar{\chi}_j^0\chi_i^+}^{L*} + C_{W^-\bar{\chi}_j^0\chi_i^+}^L C_{W^-\bar{\chi}_j^0\chi_i^+}^{R*}) P\left(\frac{-1}{12}, \frac{-5}{24}, \frac{1}{12}, \frac{-1}{144}, 1, x_t\right) + \\
& \left. (C_{W^-\bar{\chi}_j^0\chi_i^+}^R C_{W^-\bar{\chi}_j^0\chi_i^+}^{L*} - C_{W^-\bar{\chi}_j^0\chi_i^+}^L C_{W^-\bar{\chi}_j^0\chi_i^+}^{R*}) P\left(\frac{1}{16}, \frac{7}{24}, 0, 0, 1, x_t\right) \right\} \\
& + C_{W^-\bar{\chi}_i^+\chi^{++}}^{L,R} \leftrightarrow C_{W^-\bar{\chi}_j^0\chi_i^+}^{L,R}, \tag{B8}
\end{aligned}$$

$$\begin{aligned}
C_{7,NP}^{WH}(\mu_{EW}) &= \sum_{\chi_i^\pm, \chi_j^0, H_k^\pm} \frac{C_{H_k^- \bar{d}u}^L m_W^2}{4\sqrt{2}\pi^2 m_d m_f V_{ud}^*} \left\{ \left[\Re\left(C_{H_k^- \bar{\chi}_j^0\chi_i^+}^L C_{W^-\bar{\chi}_j^0\chi_i^+}^L + C_{H_k^- \bar{\chi}_j^0\chi_i^+}^R C_{W^-\bar{\chi}_j^0\chi_i^+}^R\right) - \right. \right. \\
& i\Im\left(C_{H_k^- \bar{\chi}_j^0\chi_i^+}^L C_{W^-\bar{\chi}_j^0\chi_i^+}^L + C_{H_k^- \bar{\chi}_j^0\chi_i^+}^R C_{W^-\bar{\chi}_j^0\chi_i^+}^R\right) \left. \left(\frac{21}{64} - \frac{5}{288} + \frac{5}{24}J(m_W^2, \right. \right. \\
& \left. \left. M_{H_k^\pm}^2, m_t^2)\right) + \left[\Re\left(C_{H_k^- \bar{\chi}_j^0\chi_i^+}^L C_{W^-\bar{\chi}_j^0\chi_i^+}^R + C_{H_k^- \bar{\chi}_j^0\chi_i^+}^R C_{W^-\bar{\chi}_j^0\chi_i^+}^L\right) - \right. \\
& i\Im\left(C_{H_k^- \bar{\chi}_j^0\chi_i^+}^L C_{W^-\bar{\chi}_j^0\chi_i^+}^R + C_{H_k^- \bar{\chi}_j^0\chi_i^+}^R C_{W^-\bar{\chi}_j^0\chi_i^+}^L\right) \left. \left(\frac{-1}{144} - \frac{1}{24}J(m_W^2, \right. \right. \\
& \left. \left. M_{H_k^\pm}^2, m_t^2)\right) - \left[\Re\left(C_{H_k^- \bar{\chi}_j^0\chi_i^+}^L C_{W^-\bar{\chi}_j^0\chi_i^+}^L - C_{H_k^- \bar{\chi}_j^0\chi_i^+}^R C_{W^-\bar{\chi}_j^0\chi_i^+}^R\right) - \right. \\
& i\Im\left(C_{H_k^- \bar{\chi}_j^0\chi_i^+}^L C_{W^-\bar{\chi}_j^0\chi_i^+}^L - C_{H_k^- \bar{\chi}_j^0\chi_i^+}^R C_{W^-\bar{\chi}_j^0\chi_i^+}^R\right) \left. \left(\frac{16}{144} + \frac{1}{6}J(m_W^2, \right. \right. \\
& \left. \left. M_{H_k^\pm}^2, m_t^2)\right) - \left[\Re\left(C_{H_k^- \bar{\chi}_j^0\chi_i^+}^L C_{W^-\bar{\chi}_j^0\chi_i^+}^R - C_{H_k^- \bar{\chi}_j^0\chi_i^+}^R C_{W^-\bar{\chi}_j^0\chi_i^+}^L\right) - \right. \\
& i\Im\left(C_{H_k^- \bar{\chi}_j^0\chi_i^+}^L C_{W^-\bar{\chi}_j^0\chi_i^+}^R - C_{H_k^- \bar{\chi}_j^0\chi_i^+}^R C_{W^-\bar{\chi}_j^0\chi_i^+}^L\right) \left. \left(\frac{1}{72} + \frac{1}{12}J(m_W^2, \right. \right. \\
& \left. \left. M_{H_k^\pm}^2, m_t^2)\right) \right\} + C_{W^-(H_k^-)\bar{\chi}_i^+\chi^{++}}^{L,R} \leftrightarrow C_{W^-(H_k^-)\bar{\chi}_j^0\chi_i^+}^{L,R}, \tag{B9}
\end{aligned}$$

$$\begin{aligned}
C_{8,NP}^{WH}(\mu_{EW}) &= \sum_{\chi_i^\pm, \chi_j^0, H_k^\pm} \frac{C_{H_k^- \bar{d}u}^L m_W^2}{4\sqrt{2}\pi^2 m_d m_f V_{ud}^*} \left\{ \left[\Re\left(C_{H_k^- \bar{\chi}_j^0\chi_i^+}^L C_{W^-\bar{\chi}_j^0\chi_i^+}^L + C_{H_k^- \bar{\chi}_j^0\chi_i^+}^R C_{W^-\bar{\chi}_j^0\chi_i^+}^R\right) - \right. \right. \\
& i\Im\left(C_{H_k^- \bar{\chi}_j^0\chi_i^+}^L C_{W^-\bar{\chi}_j^0\chi_i^+}^L + C_{H_k^- \bar{\chi}_j^0\chi_i^+}^R C_{W^-\bar{\chi}_j^0\chi_i^+}^R\right) \left. \left(\frac{-1}{8\sqrt{2}}J(m_W^2, M_{H_k^\pm}^2, m_t^2)\right) + \right. \\
& \left. \left[\Re\left(C_{H_k^- \bar{\chi}_j^0\chi_i^+}^L C_{W^-\bar{\chi}_j^0\chi_i^+}^R + C_{H_k^- \bar{\chi}_j^0\chi_i^+}^R C_{W^-\bar{\chi}_j^0\chi_i^+}^L\right) + \right. \right.
\end{aligned}$$

$$\begin{aligned}
& i\mathfrak{S}\left(C_{H_k^- \bar{\chi}_j^0 \chi_i^+}^L C_{W^- \bar{\chi}_j^0 \chi_i^+}^R + C_{H_k^- \bar{\chi}_j^0 \chi_i^+}^R C_{W^- \bar{\chi}_j^0 \chi_i^+}^L\right) \left(\frac{-1}{8\sqrt{2}} J(m_W^2, M_{H_k^\pm}^2, m_t^2)\right) + \\
& \left[\Re\left(C_{H_k^- \bar{\chi}_j^0 \chi_i^+}^L C_{W^- \bar{\chi}_j^0 \chi_i^+}^L - C_{H_k^- \bar{\chi}_j^0 \chi_i^+}^R C_{W^- \bar{\chi}_j^0 \chi_i^+}^R\right) - \right. \\
& i\mathfrak{S}\left(C_{H_k^- \bar{\chi}_j^0 \chi_i^+}^L C_{W^- \bar{\chi}_j^0 \chi_i^+}^L - C_{H_k^- \bar{\chi}_j^0 \chi_i^+}^R C_{W^- \bar{\chi}_j^0 \chi_i^+}^R\right) \left(\frac{-1}{4\sqrt{2}} J(m_W^2, M_{H_k^\pm}^2, m_t^2)\right) + \\
& \left[\Re\left(C_{H_k^- \bar{\chi}_j^0 \chi_i^+}^L C_{W^- \bar{\chi}_j^0 \chi_i^+}^R + C_{H_k^- \bar{\chi}_j^0 \chi_i^+}^R C_{W^- \bar{\chi}_j^0 \chi_i^+}^L\right) + \right. \\
& i\mathfrak{S}\left(C_{H_k^- \bar{\chi}_j^0 \chi_i^+}^L C_{W^- \bar{\chi}_j^0 \chi_i^+}^R + C_{H_k^- \bar{\chi}_j^0 \chi_i^+}^R C_{W^- \bar{\chi}_j^0 \chi_i^+}^L\right) \left(\frac{1}{4\sqrt{2}} J(m_W^2, \right. \\
& \left. M_{H_k^\pm}^2, m_t^2)\right) \left. \right\} + C_{W^-(H_k^-) \bar{\chi}_i^+ \chi^{++}}^{L,R} \leftrightarrow C_{W^-(H_k^-) \bar{\chi}_j^0 \chi_i^+}^{L,R}. \tag{B10}
\end{aligned}$$

The concrete expressions for P and J are given by:

$$\begin{aligned}
\rho_{i,j}(x_1, x_2) &= \frac{x_1^i \ln^j x_1 - x_2^i \ln^j x_2}{x_1 - x_2}, \\
P(y_1, y_2, y_3, y_4, x_1, x_2) &= y_1 \frac{\partial \rho_{1,1}(x_1, x_2)}{\partial x_1} + y_2 \frac{\partial^2 \rho_{2,1}(x_1, x_2)}{\partial x_1^2} + \\
& y_3 \frac{\partial^3 \rho_{3,1}(x_1, x_2)}{\partial x_1^3} + y_4 \frac{\partial^4 \rho_{4,1}(x_1, x_2)}{\partial x_1^4}, \\
J(x_1, x_2, x_3) &= \ln m_F^2 - \frac{\rho_{2,1}(x_1, x_3) - \rho_{2,2}(x_2, x_3)}{x_1^2 - x_2^2}, \tag{B11}
\end{aligned}$$

where m_F runs all $m_{\chi_i^\pm}, m_{\chi_j^0}$.

The one loop Wilson coefficients for the process $B_s^0 \rightarrow \mu^+ \mu^-$ are written as

$$\begin{aligned}
C_{S,NP}^{(1)}(\mu_{EW}) &= \sum_{\tilde{U}_i, \bar{\chi}_j^-, \chi_k^-, S=h_l, A_l} \frac{C_{\mu^- S \mu^+}^L + C_{\mu^- S \mu^+}^R}{2(m_b^2 - m_S^2)} \left[C_{\tilde{U}_i \bar{s} \chi_j^-}^R C_{\bar{\chi}_j^- S \chi_k^-}^L C_{\bar{\chi}_k^- s \tilde{U}_i}^R G_2(x_{\tilde{U}_i}, x_{\chi_j^\pm}, x_{\chi_k^\pm}) \right. \\
& \left. + M_{\chi_j^\pm} M_{\chi_k^\pm} C_{\tilde{U}_i \bar{s} \chi_j^-}^R C_{\bar{\chi}_j^- S \chi_k^-}^R C_{\bar{\chi}_k^- s \tilde{U}_i}^R G_1(x_{\tilde{U}_i}, x_{\chi_j^\pm}, x_{\chi_k^\pm}) \right] \\
& + \sum_{H_i^-, u_j, u_k, S=h_l, A_l} \frac{C_{\mu^- S \mu^+}^L + C_{\mu^- S \mu^+}^R}{2(m_b^2 - m_S^2)} \left[C_{H_i^- \bar{s} u_j}^R C_{\bar{u}_j S u_k}^L C_{\bar{u}_k b H_i^-}^R G_2(x_{\tilde{H}_i^\pm}, x_{u_j}, x_{u_k}) \right. \\
& \left. + m_{u_j} m_{u_k} C_{H_i^- \bar{s} u_j}^R C_{\bar{u}_j S u_k}^R C_{\bar{u}_k b H_i^-}^R G_1(x_{\tilde{H}_i^\pm}, x_{u_j}, x_{u_k}) \right], \\
C_{P,NP}^{(1)}(\mu_{EW}) &= \sum_{\tilde{U}_i, \bar{\chi}_j^-, \chi_k^-, S=h_l, A_l} \frac{-C_{\mu^- S \mu^+}^L + C_{\mu^- S \mu^+}^R}{2(m_b^2 - m_S^2)} \left[C_{\tilde{U}_i \bar{s} \chi_j^-}^R C_{\bar{\chi}_j^- S \chi_k^-}^L C_{\bar{\chi}_k^- s \tilde{U}_i}^R G_2(x_{\tilde{U}_i}, x_{\chi_j^\pm}, x_{\chi_k^\pm}) \right. \\
& \left. + M_{\chi_j^\pm} M_{\chi_k^\pm} C_{\tilde{U}_i \bar{s} \chi_j^-}^R C_{\bar{\chi}_j^- S \chi_k^-}^R C_{\bar{\chi}_k^- s \tilde{U}_i}^R G_1(x_{\tilde{U}_i}, x_{\chi_j^\pm}, x_{\chi_k^\pm}) \right] \\
& + \sum_{H_i^-, u_j, u_k, S=h_l, A_l} \frac{-C_{\mu^- S \mu^+}^L + C_{\mu^- S \mu^+}^R}{2(m_b^2 - m_S^2)} \left[C_{H_i^- \bar{s} u_j}^R C_{\bar{u}_j S u_k}^L C_{\bar{u}_k b H_i^-}^R G_2(x_{\tilde{H}_i^\pm}, x_{u_j}, x_{u_k}) \right. \\
& \left. + m_{u_j} m_{u_k} C_{H_i^- \bar{s} u_j}^R C_{\bar{u}_j S u_k}^R C_{\bar{u}_k b H_i^-}^R G_1(x_{\tilde{H}_i^\pm}, x_{u_j}, x_{u_k}) \right], \tag{B12}
\end{aligned}$$

$$\begin{aligned}
C_{S,NP}^{(2)}(\mu_{EW}) &= \sum_{u_i, H_j^\pm, H_k^\pm, S=h_l, A_l} \frac{1}{2(m_b^2 - m_S^2)} m_{u_i} C_{\bar{s}u_i H_j^\pm}^R C_{\bar{u}_i b H_k^\pm}^R C_{SH_j^\pm H_k^\pm} C_{SH_j^\pm H_k^\pm} G_1(x_{u_i}, x_{H_j^\pm}, x_{H_k^\pm}) \\
&\quad (C_{\mu^- S \mu^+}^L + C_{\mu^- S \mu^+}^R) \\
&\quad + \sum_{\chi_i^\pm, \tilde{U}_j, \tilde{U}_k, S=h_l, A_l} \frac{1}{2(m_b^2 - m_S^2)} m_{\chi_i^\pm} C_{\bar{s}\chi_i^\pm \tilde{U}_j}^R C_{\bar{\chi}_i^\pm b \tilde{U}_k}^R C_{S\tilde{U}_j \tilde{U}_k} G_1(x_{\chi_i^\pm}, x_{\tilde{U}_j}, x_{\tilde{U}_k}) \\
&\quad (C_{\mu^- S \mu^+}^L + C_{\mu^- S \mu^+}^R), \\
C_{P,NP}^{(2)}(\mu_{EW}) &= \sum_{u_i, H_j^\pm, H_k^\pm, S=h_l, A_l} \frac{1}{2(m_b^2 - m_S^2)} m_{u_i} C_{\bar{s}u_i H_j^\pm}^R C_{\bar{u}_i b H_k^\pm}^R C_{SH_j^\pm H_k^\pm} G_1(x_{u_i}, x_{H_j^\pm}, x_{H_k^\pm}) \\
&\quad (-C_{\mu^- S \mu^+}^L + C_{\mu^- S \mu^+}^R) \\
&\quad + \sum_{\chi_i^\pm, \tilde{U}_j, \tilde{U}_k, S=h_l, A_l} \frac{1}{2(m_b^2 - m_S^2)} m_{\chi_i^\pm} C_{\bar{s}\chi_i^\pm \tilde{U}_j}^R C_{\bar{\chi}_i^\pm b \tilde{U}_k}^R C_{S\tilde{U}_j \tilde{U}_k} G_1(x_{\chi_i^\pm}, x_{\tilde{U}_j}, x_{\tilde{U}_k}) \\
&\quad (-C_{\mu^- S \mu^+}^L + C_{\mu^- S \mu^+}^R), \tag{B13}
\end{aligned}$$

$$\begin{aligned}
C_{S,NP}^{(3)}(\mu_{EW}) &= \sum_{u_i, H_k^\pm, S=h_l, A_l} \frac{-C_{W^\pm SH_k^\pm}}{2(m_b^2 - m_S^2)} \left[C_{\bar{s}W^\pm u_i}^L C_{\bar{u}_i H_k^\pm b}^R G_2(x_{u_i}, 1, x_{H_k^\pm}) - 2m_b m_{u_i} C_{\bar{s}W^\pm u_i}^L \right. \\
&\quad \left. C_{\bar{u}_i H_k^\pm b}^L G_1(x_{u_i}, 1, x_{H_k^\pm}) \right] (C_{\mu^- S \mu^+}^L + C_{\mu^- S \mu^+}^R), \\
C_{P,NP}^{(3)}(\mu_{EW}) &= \sum_{u_i, H_k^\pm, S=h_l, A_l} \frac{-C_{W^\pm SH_k^\pm}}{2(m_b^2 - m_S^2)} \left[C_{\bar{s}W^\pm u_i}^L C_{\bar{u}_i H_k^\pm b}^R G_2(x_{u_i}, 1, x_{H_k^\pm}) - 2m_b m_{u_i} C_{\bar{s}W^\pm u_i}^L \right. \\
&\quad \left. C_{\bar{u}_i H_k^\pm b}^L G_1(x_{u_i}, 1, x_{H_k^\pm}) \right] (-C_{\mu^- S \mu^+}^L + C_{\mu^- S \mu^+}^R), \tag{B14}
\end{aligned}$$

$$\begin{aligned}
C_{S,NP}^{(4)}(\mu_{EW}) &= \sum_{u_i, H_j^\pm, S=h_l, A_l} \frac{-C_{W^\pm SH_j^\pm}}{2(m_b^2 - m_S^2)} C_{\bar{s}H_j^\pm u_i}^R C_{\bar{u}_i W^\pm b}^R G_2(x_{u_i}, x_{H_j^\pm}, 1) (C_{\mu^- S \mu^+}^L + C_{\mu^- S \mu^+}^R), \\
C_{S,NP}^{(4)}(\mu_{EW}) &= \sum_{u_i, H_j^\pm, S=h_l, A_l} \frac{-C_{W^\pm SH_j^\pm}}{2(m_b^2 - m_S^2)} C_{\bar{s}H_j^\pm u_i}^R C_{\bar{u}_i W^\pm b}^R G_2(x_{u_i}, x_{H_j^\pm}, 1) (-C_{\mu^- S \mu^+}^L + C_{\mu^- S \mu^+}^R), \tag{B15}
\end{aligned}$$

$$\begin{aligned}
C_{9,NP}^{(5)}(\mu_{EW}) &= \sum_{\tilde{U}_i, \chi_j^-, \chi_k^-, V} \frac{C_{\mu^- V \mu^+}^L + C_{\mu^- V \mu^+}^R}{-2(m_b^2 - m_V^2)} \left[-\frac{1}{2} C_{\tilde{U}_i \bar{s} \chi_j^-}^R C_{\bar{\chi}_j^- V \chi_k^-}^R C_{\bar{\chi}_k^- s \tilde{U}_i}^L G_2(x_{\tilde{U}_i}, x_{\chi_j^\pm}, x_{\chi_k^\pm}) \right. \\
&\quad \left. + M_{\chi_j^\pm} M_{\chi_k^\pm} C_{\tilde{U}_i \bar{s} \chi_j^-}^R C_{\bar{\chi}_j^- V \chi_k^-}^L C_{\bar{\chi}_k^- s \tilde{U}_i}^L G_1(x_{\tilde{U}_i}, x_{\chi_j^\pm}, x_{\chi_k^\pm}) \right] \\
&\quad + \sum_{\tilde{H}_i^\pm, u_j, u_k, V} \frac{C_{\mu^- V \mu^+}^L + C_{\mu^- V \mu^+}^R}{-2(m_b^2 - m_V^2)} \left[-\frac{1}{2} C_{H_i^\pm \bar{s} u_j}^R C_{\bar{u}_j V u_k}^R C_{u_k s H_i^\pm}^L G_2(x_{H_i^\pm}, x_{u_j}, x_{u_k}) \right.
\end{aligned}$$

$$\begin{aligned}
& +m_{u_j}m_{u_k}C_{H_i^\pm\bar{s}u_j}^RC_{\bar{u}_jV u_k}^LC_{\bar{u}_k s H_i^\pm}^LG_1(x_{H_i^\pm}, x_{u_j}, x_{u_k}), \\
C_{10,NP}^{(5)}(\mu_{EW}) = & \sum_{\tilde{u}_i, \chi_j^-, \chi_k^-, V} \frac{-C_{\mu^-V\mu^+}^L + C_{\mu^-V\mu^+}^R}{-2(m_b^2 - m_V^2)} \left[-\frac{1}{2}C_{\tilde{U}_i\bar{s}\chi_j^-}^RC_{\bar{\chi}_j^-V\chi_k^-}^RC_{\bar{\chi}_k^-s\tilde{U}_i}^LG_2(x_{\tilde{U}_i}, x_{\chi_j^\pm}, x_{\chi_k^\pm}) \right. \\
& + M_{\chi_j^\pm}M_{\chi_k^\pm}C_{\tilde{U}_i\bar{s}\chi_j^-}^RC_{\bar{\chi}_j^-V\chi_k^-}^LC_{\bar{\chi}_k^-s\tilde{U}_i}^LG_1(x_{\tilde{U}_i}, x_{\chi_j^\pm}, x_{\chi_k^\pm}) \left. \right] \\
& + \sum_{\tilde{H}_i^\pm, u_j, u_k, V} \frac{-C_{\mu^-V\mu^+}^L + C_{\mu^-V\mu^+}^R}{-2(m_b^2 - m_V^2)} \left[-\frac{1}{2}C_{H_i^\pm\bar{s}u_j}^RC_{\bar{u}_jV u_k}^RC_{u_k s H_i^\pm}^LG_2(x_{H_i^\pm}, x_{u_j}, x_{u_k}) \right. \\
& \left. + m_{u_j}m_{u_k}C_{H_i^\pm\bar{s}u_j}^RC_{\bar{u}_jV u_k}^LC_{\bar{u}_k s H_i^\pm}^LG_1(x_{H_i^\pm}, x_{u_j}, x_{u_k}) \right], \tag{B16}
\end{aligned}$$

$$\begin{aligned}
C_{9,NP}^{(6)}(\mu_{EW}) = & \sum_{u_i, H_j^\pm, H_k^\pm, V} \frac{C_{\mu^-V\mu^+}^L + C_{\mu^-V\mu^+}^R}{4(m_b^2 - m_V^2)} C_{\bar{s}u_i H_j^\pm}^RC_{\bar{u}_i b H_k^\pm}^LC_{V H_j^\pm H_k^\pm}^CG_2(x_{u_i}, x_{H_j^\pm}, x_{H_k^\pm}) \\
& + \sum_{\chi_i^\pm, \tilde{U}_j, \tilde{U}_k, V} \frac{C_{\mu^-V\mu^+}^L + C_{\mu^-V\mu^+}^R}{4(m_b^2 - m_V^2)} C_{\bar{s}\chi_i^\pm\tilde{U}_j}^RC_{\bar{\chi}_i^\pm b\tilde{U}_k}^LC_{V\tilde{U}_j\tilde{U}_k}^CG_2(x_{\chi_i^\pm}, x_{\tilde{U}_j}, x_{\tilde{U}_k}), \\
C_{10,NP}^{(6)}(\mu_{EW}) = & \sum_{u_i, H_j^\pm, H_k^\pm, V} \frac{-C_{\mu^-V\mu^+}^L + C_{\mu^-V\mu^+}^R}{4(m_b^2 - m_V^2)} C_{\bar{s}u_i H_j^\pm}^RC_{\bar{u}_i b H_k^\pm}^LC_{V H_j^\pm H_k^\pm}^CG_2(x_{u_i}, x_{H_j^\pm}, x_{H_k^\pm}) \\
& + \sum_{\chi_i^\pm, \tilde{U}_j, \tilde{U}_k, V} \frac{-C_{\mu^-V\mu^+}^L + C_{\mu^-V\mu^+}^R}{4(m_b^2 - m_V^2)} C_{\bar{s}\chi_i^\pm\tilde{U}_j}^RC_{\bar{\chi}_i^\pm b\tilde{U}_k}^LC_{V\tilde{U}_j\tilde{U}_k}^CG_2(x_{\chi_i^\pm}, x_{\tilde{U}_j}, x_{\tilde{U}_k}), \\
C_{S,NP}^{(6)}(\mu_{EW}) = & \sum_{u_i, H_j^\pm, H_k^\pm, V} \frac{C_{\mu^-V\mu^+}^L + C_{\mu^-V\mu^+}^R}{-2(m_b^2 - m_V^2)} m_b m_{u_i} C_{\bar{s}u_i H_j^\pm}^RC_{\bar{u}_i b H_k^\pm}^RC_{V H_j^\pm H_k^\pm}^CG_1(x_{u_i}, x_{H_j^\pm}, x_{H_k^\pm}) \\
& + \sum_{\chi_i^\pm, \tilde{U}_j, \tilde{U}_k, V} \frac{C_{\mu^-V\mu^+}^L + C_{\mu^-V\mu^+}^R}{-2(m_b^2 - m_V^2)} m_b m_{\chi_i^\pm} C_{\bar{s}\chi_i^\pm\tilde{U}_j}^RC_{\bar{\chi}_i^\pm b\tilde{U}_k}^RC_{V\tilde{U}_j\tilde{U}_k}^CG_1(x_{\chi_i^\pm}, x_{\tilde{U}_j}, x_{\tilde{U}_k}), \\
C_{P,NP}^{(6)}(\mu_{EW}) = & \sum_{u_i, H_j^\pm, H_k^\pm, V} \frac{C_{\mu^-V\mu^+}^L - C_{\mu^-V\mu^+}^R}{-2(m_b^2 - m_V^2)} m_b m_{u_i} C_{\bar{s}u_i H_j^\pm}^RC_{\bar{u}_i b H_k^\pm}^RC_{V H_j^\pm H_k^\pm}^CG_1(x_{u_i}, x_{H_j^\pm}, x_{H_k^\pm}) \\
& + \sum_{\chi_i^\pm, \tilde{U}_j, \tilde{U}_k, V} \frac{C_{\mu^-V\mu^+}^L - C_{\mu^-V\mu^+}^R}{-2(m_b^2 - m_V^2)} m_b m_{\chi_i^\pm} C_{\bar{s}\chi_i^\pm\tilde{U}_j}^RC_{\bar{\chi}_i^\pm b\tilde{U}_k}^RC_{V\tilde{U}_j\tilde{U}_k}^CG_1(x_{\chi_i^\pm}, x_{\tilde{U}_j}, x_{\tilde{U}_k}), \tag{B17}
\end{aligned}$$

$$C_{9,NP}^{(7)}(\mu_{EW}) = \sum_{u_i, H_k^\pm, V} \frac{C_{\mu^-V\mu^+}^L + C_{\mu^-V\mu^+}^R}{2(m_b^2 - m_V^2)} m_{u_i} C_{\bar{s}u_i W^\pm}^LC_{\bar{u}_i b H_k^\pm}^LC_{V W^\pm H_k^\pm}^CG_1(x_{u_i}, x_W, x_{H_k^\pm}),$$

$$C_{10,NP}^{(7)}(\mu_{EW}) = \sum_{u_i, H_k^\pm, V} \frac{-C_{\mu^-V\mu^+}^L + C_{\mu^-V\mu^+}^R}{2(m_b^2 - m_V^2)} m_{u_i} C_{\bar{s}u_i W^\pm}^LC_{\bar{u}_i b H_k^\pm}^LC_{V W^\pm H_k^\pm}^CG_1(x_{u_i}, x_W, x_{H_k^\pm}),$$

(B18)

$$\begin{aligned}
C_{9,NP}^{(8)}(\mu_{EW}) &= \sum_{u_i, H_j^\pm, V} \frac{C_{\mu^- V \mu^+}^L + C_{\mu^- V \mu^+}^R}{2(m_b^2 - m_V^2)} m_{u_i} C_{\bar{s}u_i H_j^\pm}^R C_{\bar{u}_i b W^\pm}^L C_{VW^\pm H_k^\pm} G_1(x_{u_i}, x_{H_j^\pm}, x_W), \\
C_{10,NP}^{(8)}(\mu_{EW}) &= \sum_{u_i, H_j^\pm, V} \frac{-C_{\mu^- V \mu^+}^L + C_{\mu^- V \mu^+}^R}{2(m_b^2 - m_V^2)} m_{u_i} C_{\bar{s}u_i H_j^\pm}^R C_{\bar{u}_i b W^\pm}^L C_{VW^\pm H_k^\pm} G_1(x_{u_i}, x_{H_j^\pm}, x_W),
\end{aligned} \tag{B19}$$

$$\begin{aligned}
C_{9,NP}^{(9)}(\mu_{EW}) &= \sum_{\tilde{U}_i, \chi_j^\pm, \chi_k^\pm, \tilde{\nu}_l} -\frac{1}{8} C_{\bar{s}\tilde{U}_i \chi_j^\pm}^R C_{\bar{\chi}_j^\pm \mu^+ \tilde{\nu}_l}^L (C_{\mu^- \tilde{\nu}_l \chi_k^\pm}^L C_{\bar{\chi}_k^\pm \tilde{U}_i b}^R + C_{\mu^- \tilde{\nu}_l \chi_k^\pm}^R C_{\bar{\chi}_k^\pm \tilde{U}_i b}^L) \\
&\quad G_4(x_{\tilde{U}_i}, x_{\chi_j^\pm}, x_{\chi_k^\pm}, x_{\tilde{\nu}_l}), \\
C_{10,NP}^{(9)}(\mu_{EW}) &= \sum_{\tilde{U}_i, \chi_j^\pm, \chi_k^\pm, \tilde{\nu}_l} -\frac{1}{8} C_{\bar{s}\tilde{U}_i \chi_j^\pm}^R C_{\bar{\chi}_j^\pm \mu^+ \tilde{\nu}_l}^L (C_{\mu^- \tilde{\nu}_l \chi_k^\pm}^L C_{\bar{\chi}_k^\pm \tilde{U}_i b}^R - C_{\mu^- \tilde{\nu}_l \chi_k^\pm}^R C_{\bar{\chi}_k^\pm \tilde{U}_i b}^L) \\
&\quad G_4(x_{\tilde{U}_i}, x_{\chi_j^\pm}, x_{\chi_k^\pm}, x_{\tilde{\nu}_l}), \\
C_{S,NP}^{(9)}(\mu_{EW}) &= \sum_{\tilde{U}_i, \chi_j^\pm, \chi_k^\pm, \tilde{\nu}_l} -\frac{1}{2} M_{\chi_j^\pm} M_{\chi_k^\pm} C_{\bar{s}\tilde{U}_i \chi_j^\pm}^R C_{\bar{\chi}_j^\pm \mu^+ \tilde{\nu}_l}^L (C_{\mu^- \tilde{\nu}_l \chi_k^\pm}^L C_{\bar{\chi}_k^\pm \tilde{U}_i b}^L + C_{\mu^- \tilde{\nu}_l \chi_k^\pm}^R C_{\bar{\chi}_k^\pm \tilde{U}_i b}^R) \\
&\quad G_3(x_{\tilde{U}_i}, x_{\chi_j^\pm}, x_{\chi_k^\pm}, x_{\tilde{\nu}_l}), \\
C_{P,NP}^{(9)}(\mu_{EW}) &= \sum_{\tilde{U}_i, \chi_j^\pm, \chi_k^\pm, \tilde{\nu}_l} -\frac{1}{2} M_{\chi_j^\pm} M_{\chi_k^\pm} C_{\bar{s}\tilde{U}_i \chi_j^\pm}^R C_{\bar{\chi}_j^\pm \mu^+ \tilde{\nu}_l}^L (-C_{\mu^- \tilde{\nu}_l \chi_k^\pm}^L C_{\bar{\chi}_k^\pm \tilde{U}_i b}^L + C_{\mu^- \tilde{\nu}_l \chi_k^\pm}^R C_{\bar{\chi}_k^\pm \tilde{U}_i b}^R) \\
&\quad G_3(x_{\tilde{U}_i}, x_{\chi_j^\pm}, x_{\chi_k^\pm}, x_{\tilde{\nu}_l}),
\end{aligned} \tag{B20}$$

$$\begin{aligned}
C_{9,NP}^{(10)}(\mu_{EW}) &= \sum_{u_i, H_j^\pm, H_k^\pm, \tilde{\nu}_l} \frac{1}{8} C_{\bar{s}u_i H_j^\pm}^R C_{\bar{u}_i b H_k^\pm}^L (C_{\mu^- H_k^\pm \nu_l}^L C_{\tilde{\nu}_l H_j^\pm \mu^+}^R + C_{\mu^- H_k^\pm \nu_l}^R C_{\tilde{\nu}_l H_j^\pm \mu^+}^L) \\
&\quad G_4(x_{u_i}, x_{H_j^\pm}, x_{H_k^\pm}, x_{\nu_l}), \\
C_{10,NP}^{(10)}(\mu_{EW}) &= \sum_{u_i, H_j^\pm, H_k^\pm, \tilde{\nu}_l} \frac{1}{8} C_{\bar{s}u_i H_j^\pm}^R C_{\bar{u}_i b H_k^\pm}^L (C_{\mu^- H_k^\pm \nu_l}^L C_{\tilde{\nu}_l H_j^\pm \mu^+}^R - C_{\mu^- H_k^\pm \nu_l}^R C_{\tilde{\nu}_l H_j^\pm \mu^+}^L) \\
&\quad G_4(x_{u_i}, x_{H_j^\pm}, x_{H_k^\pm}, x_{\nu_l}),
\end{aligned} \tag{B21}$$

$$\begin{aligned}
C_{S,NP}^{(11)}(\mu_{EW}) &= - \sum_{u_i, H_j^\pm, \nu_l} \frac{1}{2} C_{\bar{s}u_i H_j^\pm}^R C_{\bar{u}_i b W^\pm}^R C_{\mu^- W^\pm \nu_l}^R C_{\tilde{\nu}_l H_j^\pm \mu^+}^L G_4(x_{u_i}, x_{H_j^\pm}, x_W, x_{\nu_l}), \\
C_{P,NP}^{(11)}(\mu_{EW}) &= - \sum_{u_i, H_j^\pm, \nu_l} \frac{1}{2} C_{\bar{s}u_i H_j^\pm}^R C_{\bar{u}_i b W^\pm}^R C_{\mu^- W^\pm \nu_l}^R C_{\tilde{\nu}_l H_j^\pm \mu^+}^L G_4(x_{u_i}, x_{H_j^\pm}, x_W, x_{\nu_l}),
\end{aligned} \tag{B22}$$

where V denotes photon γ , Z boson and C_{iVt} , $C_{\bar{\chi}_j^0 V \chi_j^0}$, $C_{\bar{\chi}_i^+ V \chi_i^+}$ denote the vector parts of the corresponding interaction vertex.

The two loop Wilson coefficients for the process $B_s^0 \rightarrow \mu^+ \mu^-$ are written as

$$\begin{aligned}
C_{9,NP}^{WW}(\mu_{EW}) = & \sum_{\chi_i^+, \chi_j^0, V} \frac{(C_{\mu^- V \mu^+}^R + C_{\mu^- V \mu^+}^L) g_s^2}{128 \pi^4 s_W^2} \frac{m_b^2}{m_b^2 - m_V^2} \left\{ \left[(|C_{W^- \bar{\chi}_j^0 \chi_i^+}^L|^2 + |C_{W^- \bar{\chi}_j^0 \chi_i^+}^R|^2) \right. \right. \\
& P\left(\frac{1}{8}, \frac{1}{4}, \frac{-1}{48}, \frac{-1}{144}, 1, x_t\right) + (|C_{W^- \bar{\chi}_j^0 \chi_i^+}^L|^2 - |C_{W^- \bar{\chi}_j^0 \chi_i^+}^R|^2) \frac{\partial^1 \rho_{1,1}}{\partial x_1} (x_W, x_t) + \\
& (C_{W^- \bar{\chi}_j^0 \chi_i^+}^R C_{W^- \bar{\chi}_j^0 \chi_i^+}^{L*} + C_{W^- \bar{\chi}_j^0 \chi_i^+}^L C_{W^- \bar{\chi}_j^0 \chi_i^+}^{R*}) P\left(\frac{1}{16}, \frac{1}{4}, \frac{-1}{16}, \frac{1}{144}, 1, x_t\right) + \\
& \left. \frac{1}{8} (C_{W^- \bar{\chi}_j^0 \chi_i^+}^L C_{W^- \bar{\chi}_j^0 \chi_i^+}^{R*} - C_{W^- \bar{\chi}_j^0 \chi_i^+}^R C_{W^- \bar{\chi}_j^0 \chi_i^+}^{L*}) \frac{\partial^2 \rho_{2,1}}{\partial x_1^2} (x_W, x_t) \right] C_{VW-W-} + \\
& \left[(|C_{W^- \bar{\chi}_j^0 \chi_i^+}^L|^2 + |C_{W^- \bar{\chi}_j^0 \chi_i^+}^R|^2) P\left(\frac{1}{144}, \frac{-1}{12}, \frac{-29}{72}, \frac{-11}{12}, 1, x_t\right) + (C_{W^- \bar{\chi}_j^0 \chi_i^+}^R \right. \\
& C_{W^- \bar{\chi}_j^0 \chi_i^+}^{L*} + C_{W^- \bar{\chi}_j^0 \chi_i^+}^L C_{W^- \bar{\chi}_j^0 \chi_i^+}^{R*}) P\left(\frac{-1}{144}, \frac{1}{12}, \frac{-5}{24}, \frac{-1}{12}, 1, x_t\right) \left. \right] C_{iVt} + \\
& \left[(|C_{W^- \bar{\chi}_j^0 \chi_i^+}^L|^2 + |C_{W^- \bar{\chi}_j^0 \chi_i^+}^R|^2) P\left(\frac{3}{16}, \frac{3}{16}, 0, 0, 1, x_t\right) + \frac{1}{16} (C_{W^- \bar{\chi}_j^0 \chi_i^+}^L \right. \\
& C_{W^- \bar{\chi}_j^0 \chi_i^+}^{R*} - C_{W^- \bar{\chi}_j^0 \chi_i^+}^R C_{W^- \bar{\chi}_j^0 \chi_i^+}^{L*}) \frac{\partial^2 \rho_{2,1}}{\partial x_1^2} (x_W, x_t) \left. \right] (C_{\bar{\chi}_j^0 V \chi_j^0} + C_{\bar{\chi}_i^+ V \chi_i^+}) \left. \right\} \\
& + C_{W^- \bar{\chi}_i^+ \chi^{++}}^{L,R} \leftrightarrow C_{W^- \bar{\chi}_j^0 \chi_i^+}^{L,R}, \tag{B23}
\end{aligned}$$

$$\begin{aligned}
C_{10,NP}^{WW}(\mu_{EW}) = & \sum_{\chi_i^+, \chi_j^0, V} \frac{(C_{\mu^- V \mu^+}^R - C_{\mu^- V \mu^+}^L) g_s^2}{128 \pi^4 s_W^2} \frac{m_b^2}{m_b^2 - m_V^2} \left\{ \left[(|C_{W^- \bar{\chi}_j^0 \chi_i^+}^L|^2 + |C_{W^- \bar{\chi}_j^0 \chi_i^+}^R|^2) \right. \right. \\
& P\left(\frac{1}{8}, \frac{1}{4}, \frac{-1}{48}, \frac{-1}{144}, 1, x_t\right) + (|C_{W^- \bar{\chi}_j^0 \chi_i^+}^L|^2 - |C_{W^- \bar{\chi}_j^0 \chi_i^+}^R|^2) \frac{\partial^1 \rho_{1,1}}{\partial x_1} (x_W, x_t) + \\
& (C_{W^- \bar{\chi}_j^0 \chi_i^+}^R C_{W^- \bar{\chi}_j^0 \chi_i^+}^{L*} + C_{W^- \bar{\chi}_j^0 \chi_i^+}^L C_{W^- \bar{\chi}_j^0 \chi_i^+}^{R*}) P\left(\frac{1}{16}, \frac{1}{4}, \frac{-1}{16}, \frac{1}{144}, 1, x_t\right) + \\
& \left. \frac{1}{8} (C_{W^- \bar{\chi}_j^0 \chi_i^+}^L C_{W^- \bar{\chi}_j^0 \chi_i^+}^{R*} - C_{W^- \bar{\chi}_j^0 \chi_i^+}^R C_{W^- \bar{\chi}_j^0 \chi_i^+}^{L*}) \frac{\partial^2 \rho_{2,1}}{\partial x_1^2} (x_W, x_t) \right] C_{VW-W-} + \\
& \left[(|C_{W^- \bar{\chi}_j^0 \chi_i^+}^L|^2 + |C_{W^- \bar{\chi}_j^0 \chi_i^+}^R|^2) P\left(\frac{1}{144}, \frac{-1}{12}, \frac{-29}{72}, \frac{-11}{12}, 1, x_t\right) + (C_{W^- \bar{\chi}_j^0 \chi_i^+}^R \right. \\
& C_{W^- \bar{\chi}_j^0 \chi_i^+}^{L*} + C_{W^- \bar{\chi}_j^0 \chi_i^+}^L C_{W^- \bar{\chi}_j^0 \chi_i^+}^{R*}) P\left(\frac{-1}{144}, \frac{1}{12}, \frac{-5}{24}, \frac{-1}{12}, 1, x_t\right) \left. \right] C_{iVt} + \\
& \left[(|C_{W^- \bar{\chi}_j^0 \chi_i^+}^L|^2 + |C_{W^- \bar{\chi}_j^0 \chi_i^+}^R|^2) P\left(\frac{3}{16}, \frac{3}{16}, 0, 0, 1, x_t\right) + \frac{1}{16} (C_{W^- \bar{\chi}_j^0 \chi_i^+}^L \right. \\
& C_{W^- \bar{\chi}_j^0 \chi_i^+}^{R*} - C_{W^- \bar{\chi}_j^0 \chi_i^+}^R C_{W^- \bar{\chi}_j^0 \chi_i^+}^{L*}) \frac{\partial^2 \rho_{2,1}}{\partial x_1^2} (x_W, x_t) \left. \right] (C_{\bar{\chi}_j^0 V \chi_j^0} + C_{\bar{\chi}_i^+ V \chi_i^+}) \left. \right\} \\
& + C_{W^- \bar{\chi}_i^+ \chi^{++}}^{L,R} \leftrightarrow C_{W^- \bar{\chi}_j^0 \chi_i^+}^{L,R}. \tag{B24}
\end{aligned}$$

The concrete expressions for G_k ($k = 1, \dots, 4$) are written as

$$\begin{aligned}
G_1(x_1, x_2, x_3) &= \frac{-1}{m_W^2} \left[\frac{x_1 \ln x_1}{(x_2 - x_1)(x_3 - x_1)} + \frac{x_2 \ln x_2}{(x_1 - x_2)(x_3 - x_2)} + \frac{x_3 \ln x_3}{(x_1 - x_3)(x_2 - x_3)} \right], \\
G_2(x_1, x_2, x_3) &= -\frac{x_1^2 \ln x_1}{(x_2 - x_1)(x_3 - x_1)} - \frac{x_2^2 \ln x_2}{(x_1 - x_2)(x_3 - x_2)} - \frac{x_3^2 \ln x_3}{(x_1 - x_3)(x_2 - x_3)}, \\
G_3(x_1, x_2, x_3, x_4) &= \frac{1}{m_W^4} \left[\frac{x_1 \ln x_1}{(x_2 - x_1)(x_3 - x_1)(x_4 - x_1)} + \frac{x_2 \ln x_2}{(x_1 - x_2)(x_3 - x_2)(x_4 - x_2)} + \right. \\
&\quad \left. \frac{x_3 \ln x_3}{(x_1 - x_3)(x_2 - x_3)(x_4 - x_3)} + \frac{x_4 \ln x_4}{(x_1 - x_4)(x_2 - x_4)(x_3 - x_4)} \right], \\
G_4(x_1, x_2, x_3, x_4) &= \frac{1}{m_W^2} \left[\frac{x_1^2 \ln x_1}{(x_2 - x_1)(x_3 - x_1)(x_4 - x_1)} + \frac{x_2^2 \ln x_2}{(x_1 - x_2)(x_3 - x_2)(x_4 - x_2)} + \right. \\
&\quad \left. \frac{x_3^2 \ln x_3}{(x_1 - x_3)(x_2 - x_3)(x_4 - x_3)} + \frac{x_4^2 \ln x_4}{(x_1 - x_4)(x_2 - x_4)(x_3 - x_4)} \right].
\end{aligned} \tag{B25}$$

-
- [1] R. L. Workman *et al.* (PDG), Prog. Theor. Exp. Phys. **2022**, 083C01 (2022).
- [2] J.P. Lees *et al.*, BaBar Collaboration. Phys. Rev. Lett. **109**, 191801 (2012) [arXiv:1207.2690[hep-ex]].
- [3] J.P. Lees *et al.*, BaBar Collaboration. Phys. Rev. D **86**, 052012 (2012) [arXiv:1207.2520[hep-ex]].
- [4] T. Saito *et al.*, Belle Collaboration. Phys. Rev. D **91**, 052004 (2015) [arXiv:1411.7198[hep-ex]].
- [5] K. Adel and Y.-P. Yao, Phys. Rev. D **49**, 4945 (1994).
- [6] A. Ali and C. Greub, Phys. Lett. B **361**, 146 (1995).
- [7] C. Greub, T. Hurth and D. Wyler, Phys. Rev. D **54**, 3350 (1996).
- [8] K. Chetyrkin, M. Misiak and M. Munz, Phys. Lett. B **400**, 206 (1997).
- [9] M. Misiak *et al.*, Phys. Rev. Lett. **98**, 022002 (2007).
- [10] M. Misiak and M. Steinhauser, Nucl. Phys. B **764**, 62 (2007).
- [11] M. Misiak *et al.*, Phys. Rev. Lett. **114**, 221801 (2015) [arXiv:1503.01789[hep-ph]].
- [12] M. Czakon, P. Fiedler, T. Huber, M. Misiak, T. Schutzmeier and M. Steinhauser, JHEP **1504**, 168 (2015) [arXiv:1503.01791 [hep-ph]].
- [13] A. J. Buras, J. Girschbacher and G. Isidori, Eur. Phys. J. C **72**, 2172 (2012).

- [14] P. H. Chankowski and L. Slawianowska, Phys. Rev. D **63**, 054012 (2001) [hep-ph/0008046].
- [15] P. Colangelo, F. Giannuzzi, S. Nicotri and F. Zuo, Phys. Rev. D **88**, 115011 (2013) [arXiv:1308.0489 [hep-ph]].
- [16] C. Bobeth, T. Ewerth, F. Kruger and J. Urban, Phys. Rev. D **66**, 074021 (2002) [hep-ph/0204225].
- [17] S. Baek, Phys. Lett. B **595**, 461 (2004) [hep-ph/0406007].
- [18] M. Beneke, X. Q. Li and L. Vernazza, Eur. Phys. J. C **61**, 429 (2009) [arXiv:0901.4841 [hep-ph]].
- [19] D. Feldman, Z. Liu and P. Nath, Phys. Rev. D **81**, 117701 (2010) [arXiv:1003.0437 [hep-ph]].
- [20] R. M. Wang, Y. G. Xu, Y. L. Wang and Y. D. Yang, Phys. Rev. D **85**, 094004 (2012) [arXiv:1112.3174 [hep-ph]].
- [21] S. S. AbdusSalam and L. Velasco-Sevilla, arXiv:1707.04752 [hep-ph].
- [22] M. Ciuchini, G. Degrossi, P. Gambino and G. F. Giudice, Nucl. Phys. B **527**, 21 (1998).
- [23] P. Ciafaloni, A. Romanino and A. Strumia, Nucl. Phys. B **524**, 361 (1998).
- [24] X. G. He, T. D. Nguyen and R. R. Volkas, Phys. Rev. D **38**, 814 (1988).
- [25] W. Skiba and J. Kalinowski, Nucl. Phys. B **404**, 3 (1993).
- [26] S. R. Choudhury and N. Gaur, Phys. Lett. B **451**, 86 (1999) [hep-ph/9810307].
- [27] C. S. Huang, W. Liao, Q. S. Yan and S. H. Zhu, Phys. Rev. D **63**, 114021 (2001) [Erratum-ibid. D **64**, 059902 (2001)] [hep-ph/0006250].
- [28] A. Crivellin, A. Kokulu and C. Greub, Phys. Rev. D **87**, 094031 (2013).
- [29] A. Crivellin, M. Dario and C. Wiegand, [arXiv:1903.10440 [hep-ph]].
- [30] S. Bertolini, F. Borzumati, A. Masiero and G. Ridolfi, Nucl. Phys. B **353**, 591 (1991).
- [31] R. Barbieri and G. F. Giudice, Phys. Lett. B **309**, 86 (1993).
- [32] F. Borzumati, C. Greub, T. Hurth and D. Wyler, Phys. Rev. D **62**, 075005 (2000).
- [33] S. Prelovsek and D. Wyler, Phys. Lett. B **500**, 304 (2001).
- [34] M. Causse and J. Orloff, Eur. Phys. J. C **23**, 749 (2002).
- [35] H.-B. Zhang, G.-H. Luo, T.-F. Feng, S.-M. Zhao, T.-J. Gao and K.-S. Sun, Mod. Phys. Lett. A **29**, 1450196 (2014) [arXiv:1409.6837 [hep-ph]].
- [36] T.-F. Feng, Y.-L. Yan, H.-B. Zhang and S.-M. Zhao, Phys. Rev. D **92**, 055024 (2015).

- [37] T.-F. Feng, Y.-L. Yan, H.-B. Zhang and S.-M. Zhao, *Int. J. Mod. Phys. A* **31**, 1650092 (2016) [arXiv:1603.07578 [hep-ph]].
- [38] T.-F. Feng, J.-L. Yang, H.-B. Zhang, S.-M. Zhao and R.-F. Zhu, *Phys. Rev. D* **94**, 115034 (2016) [arXiv:1612.02094 [hep-ph]].
- [39] J.-L. Yang, T.-F. Feng, S.-M. Zhao, R.-F. Zhu, X.-Y. Yang and H.-B. Zhang, *Eur. Phys. J. C* **78**, 714 (2018).
- [40] J.-B. Chen et al, *Chin. Phys. C* **45**, 053101 (2021).
- [41] X.-X. Long et al, [arXiv:2212.14211v1 [hep-ph]].
- [42] W. N. Cottingham, H. Mehrban and I. B. Whittingham, *Phys. Rev. D* **60**, 114029 (1999).
- [43] G. Barenboim and M. Raidal, *Phys. Lett. B* **457**, 109 (1999).
- [44] J. L. Hewett and D. Wells, *Phys. Rev. D* **55**, 5549 (1997).
- [45] C. Greub, T. Hurth and D. Wyler. [arXiv:hep-ph/9912420 [hep-ph]].
- [46] T. M. Aliev and M. I. Dobroliubov, *Phys. Lett. B* **237**, 573 (1990).
- [47] A. Masiero and L. Silvestrini, *B Physics and CP Violation*, Honolulu, p. 172, (1997) [arXiv:9709244 [hep-ph]].
- [48] A. Masiero and L. Silvestrini, *Highlights of Subnuclear Physics*, Erice, p. 404, (1997) [arXiv:9711401 [hep-ph]] .
- [49] K. Agashe, A. Azatov, A. Katz and D. Kim, *Phys. Rev. D*, **84**, 115024 (2011).
- [50] U. Ellwanger, C. Hugonie, and A. M. Teixeira, *Phys. Rep.* **496**, 1 (2010).
- [51] S. Chang, R. Dermisek, J. F. Gunion, and N. Weiner, *Annu. Rev. Nucl. Part. Sci.* **58**, 75 (2008).
- [52] U. Ellwanger and C. Hugonie, *Mod. Phys. Lett. A* **22**, 1581 (2007).
- [53] B. Ananthanarayan and P. Pandita, *Phys. Lett. B* **371**, 245 (1996).
- [54] B. Ananthanarayan and P. N. Pandita, *Int. J. Mod. Phys. A* **12**, 2321 (1997).
- [55] G. Degrassi and P. Slavich, *Nucl. Phys. B* **825**, 119 (2010).
- [56] J. D. Mason, *Phys. Rev. D* **80**, 015026 (2009).
- [57] U. Ellwanger and C. Hugonie, *Phys. Lett. B* **623**, 93 (2005).
- [58] M. A. Ouahid and R. AhlLaamara, *Nucl. Phys. B* **974**, 115640 (2022).
- [59] P. Bandyopadhyay, A. Costantini, and C. Corianˆ, *Phys. Rev. D*, **94**, 055030 (2016).

- [60] P. Bandyopadhyay, K. Huitu and A. Sabanci, JHEP 1310 (2013) 091 [arXiv:1306.4530 [hep-ph]].
- [61] P. Bandyopadhyay, S. Di Chiara, K. Huitu and A. S. Keceli, JHEP 1411 (2014) 062 [arXiv:1407.4836 [hep-ph]].
- [62] F. Staub, arXiv:0806.0538.
- [63] F. Staub, Comput.Phys.Commun. **181** 1077-1086 (2010) [arXiv:0909.2863].
- [64] F. Staub, Comput.Phys.Commun. **182** 808-833 (2011) [arXiv:1002.0840].
- [65] F. Staub, Comput.Phys.Commun. **184** 1792-1809 (2013) [arXiv:1207.0906].
- [66] F. Staub, Comput.Phys.Commun. **185** 1773-1790 (2014) [arXiv:1309.7223].
- [67] M. Carena, J. R. Espinosa and C. E. M. Wagner, M. Quir Phys. Lett. B **355**, 209 (1995).
- [68] M. Carena, M. Quiros and C. E. M. Wagner, Nucl. Phys. B **461**, 407 (1996).
- [69] M. Carena, S. Gori, N.R. Shah and C. E. M. Wagner, JHEP **03**, 014 (2012)
- [70] R. Grigjanis, P. J. O'Connell, M. Sutherland and H. Navelet, Phys. Rep. **22**, 93 (1993).
- [71] G. Buchalla, A. J. Buras and M. E. Lautenbacher, Rev. Mod. Phys. **68**, 1125 (1996).
- [72] W. Altmannshofer, P. Ball, A. Bharucha, A. J. Buras, D. M. Straub and M. Wick, JHEP **0901**, 019 (2009) [arXiv:0811.1214 [hep-ph]].
- [73] L. Lin, T. F. Feng and F. Sun, Mod. Phys. Lett. A **24**, 2181-2186 (2009).
- [74] X. Y. Yang and T. F. Feng, JHEP **1005**, 059 (2010).
- [75] P. Goertz and T. Pfoh, Phys. Rev. D **84**, 095016 (2011).
- [76] A. J. Buras, L. Merlo, E. Stamou, JHEP **1108** 124 (2011).
- [77] F. Goertz, T. Pfoh, Phys. Rev. D **84** 095016 (2011).
- [78] P. Gambino, M. Misiak, Nucl. Phys. B **611** 338 (2001).
- [79] M. Czakon, U. Haisch, M. Misiak, JHEP **0703** 008 (2007).
- [80] A.J. Buras, M. Misiak, M. Müünz and S. Pokorski, Nucl. Phys. B **424** 374 (1994).
- [81] T. J. Gao, T. F. Feng, J. B. Chen, Mod. Phys. Lett. A **7** 1250011 (2012).
- [82] P. Gambino, M. Gorbahn and U. Haisch, Nucl. Phys. B **673**, 238 (2003).
- [83] CMS Collab., Phys. Lett. B, **716**, 30 (2012).
- [84] ATLAS Collab., Phys. Lett. B, **716**, 1 (2012).
- [85] P.Cox, C.C. Han, T.T. Yanagida, Phys. Rev. D **104** 075035 (2021).

- [86] M. V. Beekveld, W. Beenakker, M. Schutten, et al., *SciPost Phys.* **11** 3 (2021) [arXiv:2104.03245 [hep-ph]].
- [87] M. Chakraborti, L. Roszkowski, S. Trojanowski, *JHEP* **05** 252 (2021) [arXiv:2104.04458 [hep-ph]].
- [88] F. Wang, L. Wu, Y. Xiao, et al., *Nucl. Phys. B* **970**, 115486 (2021) [arXiv:2104.03262 [hep-ph]].
- [89] M. Chakraborti, S. Heinemeyer, I. Saha, *Eur. Phys. J. C* **81** 12 (2021) [arXiv:2104.03287 [hep-ph]].
- [90] M. Endo, K. Hamaguchi, S. Iwamoto, et al., *JHEP* **07** 075 (2021) [arXiv:2104.03217 [hep-ph]].
- [91] ATLAS Collab., *Phys. Rev. D* **87**, 012008 (2013).
- [92] CMS Collab., *JHEP* **1210**, 018 (2012).
- [93] C. S. Un and O. Ozdal, *Phys. Rev. D* **93**, 055024 (2016) [arXiv:1601.02494 [hep-ph]].
- [94] F. Domingo and U. Ellwanger, *JHEP* **0712**, 090 (2007).